ROBOTIC SYSTEMS FOR INSPECTION AND SURVEILLANCE OF CIVIL STRUCTURES

A Thesis Presented

by

Jonathan Miller

to

The Faculty of the Graduate College

of

The University of Vermont

In Partial Fulfillment of the Requirements
for the Degree of Master of Science
Specializing in Mechanical Engineering

May 2004

Accepted by the Faculty of the Graduate College, The University of Vermont, in partial fulfillment of the requirements for the degree of Master of Science specializing in Mechanical Engineering.

Thesis Examination Committee:

____ Advisor
Dryver Huston, Ph.D.

____
Jean-Guy Beliveau, Ph.D.

____ Chairperson
Adel Sadek, Ph.D.

____ Vice President for
Frances E. Carr, Ph.D. Research and Dean of the Graduate College

Date: February 13, 2004

Abstract

Structural health monitoring is a key component in maintaining a sound infrastructure. The expansion and development of urban areas, as well as the deterioration of existing infrastructure components, such as bridges, pipelines, and dams, have increased the demand for routine structural integrity assessments. While federal agencies have established guidelines regulating the inspection of these infrastructure components, evaluations often suffer from a degree of inaccuracy as a result of the inspection methods employed. Furthermore, limited human resources may decrease the thoroughness of these inspections. The application of robotic systems for structural health monitoring may provide a successful means of improving the efficiency and accuracy of structural integrity assessments by assisting human efforts. This work describes the development of an autonomous robotic system for the inspection of steel bridge girders. This system serves as a mobile platform for structural health evaluation equipment. Specifically, an analysis of visual and ultrasonic capabilities will be presented, as well as a discussion of potential future applications of such a system.

Acknowledgements

I would like to thank my advisor, Dr. Dryver Huston, for his guidance and encouragement in this project. I would like to thank my committee members, Dr. Jean-Guy Beliveau and Dr. Adel Sadek, for their interest in this work. This project was completed in collaboration with MicroStrain, Inc. of Williston, VT. Thanks to Jake Galbreath of MicroStrain, Inc. for his correspondence and support. I would like to thank Brian Esser for his assistance and advice in the design of the beam-crawler. I would also like to thank Dmitri Hudak for his help in the machine shop.

Table of Contents

List of Tables

List of Figures

Chapter 1

Chapter 2

Chapter 3

Chapter 4

Chapter 5

Chapter 1
Applications of Robotic Systems for Structural Health Monitoring

1.1 Introduction

Infrastructure Management

Structural health monitoring is a key component in maintaining a sound infrastructure. Bridges, tunnels, pipelines, and dams are all examples of large structures that require routine inspection and maintenance. Most of these structures are decades old and have had prolonged exposure to harsh environments and loads. The consequences of neglecting routine inspections range from being minor to catastrophic. Even seemingly insignificant structures such as pedestrian walkways and footbridges require an inspection schedule.

The prospect of maintaining a feasible inspection schedule for the nation's vast infrastructure may seem to be an overwhelming task. However, government organizations, such as the Federal Highway Administration (FHWA), the Office of Pipeline Safety (OPS), and the Federal Energy Regulatory Commission (FERC), have set forth explicit guidelines regarding routine inspections of highway structures, pipelines, and dams to be implemented at a regional level. It is often the responsibility of state agencies to assemble inspection crews for various structural health monitoring tasks. Inspections are performed at regular intervals depending on the type of system, its condition, and its location. Most bridges are inspected biennially, with more frequent assessments if exposure to unusually detrimental conditions (e.g., floodwaters, collisions, etc.) occurs (U.S. Government, 2002). Pipeline inspection frequency is usually determined by location. Underground systems located in High Consequence Areas (HCAs), such as cities or environmentally fragile areas, are more frequently assessed than those in low risk areas (U.S. Government, 2003). The FERC Division of Dam Safety and Inspections (D2SI) oversees the construction and maintenance of dams to ensure compliance with safety guidelines (FERC, 2003). Structural integrity is determined by means of a standardized rating system. If condition ratings are low enough, corrective action must be taken.

Even with a systematic approach, maintaining a healthy infrastructure is a formidable challenge. Structural deficiencies in ever-aging highway structures and pipeline systems become increasingly likely to occur as time passes. Additionally, urban growth and development place greater demands on these structures and systems, and create the need for further maintenance and construction. Inspections after potentially catastrophic events, such as hurricanes, earthquakes, major vehicular accidents, and sabotage, are also necessary. The effectiveness of routine inspections is limited by manpower and funding, yet the increasing need for regular assessments only places a greater strain on these two factors.

Bridges

While bridges represent only a portion of the national infrastructure, they are a critical element. Every day, nearly 4 billion vehicles cross bridges in the United States (FHWA, 2002a). Bridges are subjected to severe loads, yet they are expected to provide a safe and reliable means for transportation. Failure of any one critical member can result in catastrophe.

In 1967, the safety of the nation's bridge network was called into question when the Silver Bridge on US 35 over the Ohio River collapsed during rush hour traffic, resulting in numerous fatalities (FHWA, 2002a). The incident prompted investigations into the reasons for failure and a congressional hearing resulted in the FHWA development and implementation of the National Bridge Inspection Standards (NBIS), which was enacted as part of the Federal-Aid Highway Act of 1971.

The NBIS specifies for each state highway department the necessary inspection procedures, frequency of inspection, and qualifications of inspection personnel (U.S. Government, 2003). Visual inspection is required of most structures every two years. Bridge owners (States, cities, towns, etc.) with oversight from State transportation departments are responsible for adhering to this schedule. Records of bridge conditions are reported to the FHWA, where they are compiled for the National Bridge Inventory (NBI) database. Individuals in charge of inspection teams must either have completed a comprehensive bridge inspection training course or be registered professional engineers.

In addition to regulating inspection procedures and inspector qualifications, the bridge inspection guidelines standardize a rating system to quantify various structural health levels of three major bridge components: the deck (transportation surface), the superstructure (girders, stringers, etc.), and the substructure (abutments, piers, etc.). Condition ratings are based on a ten point system with code 9 implying excellent condition and code 0 indicating a failed condition (FHWA, 2002a). Ratings are used to indicate both the severity of the deterioration as well as the extent to which it has spread on the structural element. Ratings do not necessarily correspond to the overall bridge condition, but they do provide detailed information about specific elements.

Deficient bridges can either be categorized as structurally deficient or functionally obsolete. A structurally deficient classification is a result of either poor condition ratings or a low load capacity. A bridge may be functionally obsolete if it no longer meets the functional criteria of the system for which it was built. A lane increase of the approaching road would result in a functionally obsolete bridge. Over the past 10 years the national total of deficient bridges has hovered around 30 percent. In 2000, that total was 28.6 percent with 14.8 percent classified as structurally deficient and 13.8 percent classified as functionally obsolete (FHWA, 2002a). Thus, the majority of deficient bridges are a result of poor conditions or low load ratings.

Since its inception in 1971, the NBIS has been modified to improve inspection procedures. Originally, inspections were only regulated for Federal-aid highway bridges. However, it became clear that safety regulations were necessary for all bridges. The NBIS now applies to any bridge spanning more than 20 feet on all public roads. Unfortunate incidents also led to the modification of the NBIS. The collapse of an I-95 bridge near Greenwich, Connecticut in 1983 resulted in substantial research into the fatigue of steel connections (FHWA, 2002a). Training programs and inspection methods were revised to incorporate research results. In 1987, an I-90 bridge across the Schoharie River in New York collapsed as a result of scour (i.e., flood waters eroding soil around the central pier). The FHWA reacted by enhancing regulations for underwater inspection and scour assessment (FHWA, 2002a). These disasters provided insight into potential problems, which were previously overlooked. Although revisions were made to the NBIS to prevent recurrences, further methods for improvement and enhanced vigilance are always desired.

Bridge Inspection Methods

Inspection personnel must be highly trained to recognize specific signs of deterioration that can lead to structural failure. Any structure can have defects, which signify a loss of structural integrity, whether the structure is a highway bridge or an underground gas pipeline. Some signs of deterioration may be visually obvious such as corroding steel or large surface cracks. Other signs, such as bridge deck delamination, may require the aid of ultrasonic instruments, radar, other non-destructive methods, or invasive methods such as taking core samples. Methods of nondestructive testing are the most desirable form of inspection, as they leave the member under evaluation intact. Several forms of nondestructive evaluation for bridges exist.

Bridges are composed primarily of three materials: timber, concrete, and steel (FHWA, 2002b). These three materials have very different properties and often require unique methods of evaluation. However, some forms of inspection can be used on any type of material.

Figure 1-1. Visual inspection of steel girders (FHWA, 2001).

Visual inspection is the most basic method of nondestructive testing. While it applies only to surface inspection, it can be used to evaluate any member, regardless of material. Each material has characteristic flaws indicative of structural deterioration. Trained personnel can identify the defects unique to each type of material.

Ultrasonic inspection is another widely used form of nondestructive testing. A transducer sends high frequency sound waves through a specimen. Discontinuities in the medium reflect the signal to a receiving transducer. The magnitude and delay time of the return signal indicate the size and depth of the flaw. Thus, information about sub-surface characteristics can be obtained in a non-invasive manner. Ultrasonic testing is commonly used on timber, concrete, and steel members (FHWA, 2002b). It should be noted that reading ultrasonic signals in steel reinforced concrete can be complicated because the signal travels through the two media at different velocities. Ultrasound can also be used to determine thicknesses of steel members, and is thus a good indicator of cross sectional changes.

Figure 1-2. A portable ultrasonic sensor unit (FHWA, 2002b).

Ground Penetrating Radar (GPR) techniques are often used for bridge decks. A radar antenna can send high frequency electromagnetic pulses into a bridge deck. When the signal encounters a medium change, it will be partially reflected. Thus, GPR is useful for determining asphalt thicknesses, detecting sub-surface flaws and cracks, and examining the condition of the top flange of a box beam, which is otherwise inaccessible. Additionally, ground penetrating radar techniques may be used while traveling over a structure. The High Speed Electromagnetic Roadway Measurement and Evaluation System (HERMES) Bridge Inspector, developed by the Lawrence Livermore National Laboratory, can sample concrete bridge decks at speeds of up to 60 mph (FHWA, 2002b).

Other forms of nondestructive testing exist, but are effective only for specific materials. For example, magnetic particle inspection can be used on ferromagnetic materials to detect surface and some sub-surface defects. A magnetic field induced in a steel member will have irregularities caused by small cracks and voids near the surface. These irregularities can be detected by the use of small ferromagnetic particles applied to the surface. The particles collected by the magnetic field irregularities will form an outline of the discontinuities, indicating the size, depth, and extent of the defect. Impact-echo testing is another material specific form of evaluation. This type of nondestructive testing introduces a stress pulse to a concrete member. A transducer placed near the point of impact monitors surface displacements caused by signal reflections from irregularities within the specimen.

While advanced forms of inspection can provide valuable information about subsurface flaws that cannot be detected by visual inspection, these techniques do have certain limitations. Advanced methods are often costly due to the need for expensive equipment. Analysis and interpretation of data acquired by this equipment require a high level of operator skill, and thus create the need for advanced personnel training. While advancements have been made in developing portable and compact devices, the equipment is still somewhat bulky and often requires setup time.

Visual Inspection

Due to the cost of advanced inspection techniques, less expensive forms of nondestructive evaluation are often desired. Visual inspection is currently one of the most commonly used nondestructive evaluation techniques because it is relatively inexpensive as it requires minimal, if any, use of instruments or equipment, and it can be accomplished without data processing (FHWA, 2001). As mentioned previously, visual inspection can only detect surface defects. However, a large number of structural deficiencies have surface indicators (e.g. corrosion, concrete deterioration). Aside from a limited range of detection, visual inspection does have further drawbacks. It is extremely subjective as it depends on the inspector's training, visual acuity, and state-of-mind. Also external factors such as light intensity, structure complexity, and structure accessibility play a role in determining the effectiveness of visual inspection.

Recently, the Federal Highway Administration's Nondestructive Evaluation Validation Center (NDEVC) conducted a study to investigate the reliability of visual inspection as it relates to highway bridge inspection (FHWA, 2001). Because visual inspection is so widely practiced, assessing its validity as an effective means of assessing structural integrity provides insight into the effectiveness of bridge inspections in general. The study required bridge inspectors from various state transportation departments to complete both routine and in-depth inspections of several decommissioned test bridges. The inspectors were asked to rate the condition of several different structural elements according to the standards used in actual bridge inspections. Participants were also subject to observation during the inspection as well as interviews regarding their personal methods and procedures.

Results from the study indicated that visual inspections are completed with large variability (FHWA, 2001). Condition ratings for each element varied significantly more than those predicted by statistical models. Factors affecting variability included a reported fear of traffic, near visual acuity, color vision, light intensity, structure accessibility level, and inspector rushed level. Furthermore, in-depth inspections were

Figure 1-3. Typical access equipment for visual inspections (FHWA, 2002b).

highly ineffective for detecting defects that were expected to be identified by such inspections. In fact, in-depth inspections rarely revealed deficiencies beyond those found in routine inspections. Again factors affecting the reliability of in-depth inspections included structure complexity and accessibility, as well as inspector comfort with access equipment and heights.

These results call into question the reliability of bridge inspection procedures. While the condition rating system is an attempt to quantify observations, visual inspection remains highly subjective and dependent upon external factors.

1.2 Emerging Technologies

Robotic Inspection

Guidelines determined by federal agencies set minimum standards for inspection frequency in order to keep costs low while ensuring safe operation. Inspections can quickly consume allocated funds for several reasons. Inspectors need to be highly trained to identify subtle deficiencies, as well as operate sophisticated measuring devices. Many structures are not easily accessible and require time and expensive equipment for enabling safe inspector access. Inspections often temporarily limit the operation of a structure (e.g., lane closings on bridges). This limited operation can lead to indirect expenses caused by traffic backup and decreased productivity.

Recent advances in robotic technology may prove useful in structural health monitoring. In addition to decreasing the cost of inspection, robotic systems may be able to better quantify visual inspection procedures as well as enhance current advanced inspection methods. Robots can be deployed in locations that are inaccessible to humans, thus eliminating the need for access equipment. They can carry sophisticated instrument and sensor payloads capable of acquiring multiple types of data (visual, ultrasonic, etc.). Robots could be deployed in several locations at once, collecting data from different sites for future analysis. The ability to store data files for future analysis not only allows for remote inspection capabilities, but it also increases the productivity of highly trained personnel by maximizing their time spent on data analysis and minimizing their time spent on data acquisition. Robots could limit the need for structure closures, as they can operate without interfering with routine structure use. Visual inspection reliability could also be enhanced by robotic systems. As mentioned previously, some of the factors affecting reliability include structure accessibility, inspector visual acuity, inspector comfort with access equipment, heights, and traffic, and external factors such as wind speed and light intensity (FHWA, 2001). A robot deployed in a highly inaccessible location would not be susceptible to these factors.

Research and Development

Currently, several private companies, as well as multiple universities in collaboration with government agencies, are developing robotic systems with inspection capabilities. Many of these projects focus on enhancing visual inspection by integrating various high-resolution video cameras into robotic designs.

The California Department of Transportation (Caltrans) has been developing an aerial platform system for more efficient bridge inspections without traffic delays (Woo, 1995). The platform is capable of vertical takeoff and can position a video camera within 0.6m of a bridge element. The platform is powered remotely by means of a 30m electrical cord. Images and information are transferred from the platform to a ground station by a fiber optics cable.

The University of Virginia and Virginia Technologies, Inc. have recently developed a mobile robot platform, known as the Polecat Pro, capable of performing inspections of steel high-mast light poles (Hudson, 2002). Typically, these inspections are performed by personnel at either ground level with the use of binoculars, or at elevation via a bucket truck. These methods are often costly, time consuming, and prone

Figure 1-4. Caltrans robotic aerial inspection platform (Woo, 1995).

to inaccuracy due to incomplete surface coverage. The Polecat Pro, which is tethered to the ground, can traverse pole surfaces both vertically and circumferentially through the use of six magnetic wheels, each powered by a separate servo motor. A video camera attached to the robot can provide live and detailed visual feedback. The images displayed on a separate monitor allow for remote visual inspection.

Figure 1-5. Polecat pole crawler (Virginia Technologies, Inc.).

Many companies in the inspection-based products industry have recently focused on developing robotic inspection systems. As an example, Envirosight, Inc. has marketed a remotely controlled pipe crawler for sewage and pipeline inspection. The ROVVER®

600 is designed to navigate 6 to 36 inch diameter pipes and supply visual information via a mounted video camera (Envirosight, Inc.). The tethered robot is waterproof and can operate in damp or underwater conditions. Additionally, its relatively short length allows for enhanced maneuvering capabilities.

(a) (b)

Figure 1-6. (a) ROVVER® 600. (b) A typical image from the ROVVER® 600 (Envirosight, Inc.).

While many of the developing robotic inspection technologies primarily employ visual methods, some projects have used more sophisticated inspection techniques. The Army Corps of Engineers has recently been interested in deploying robotic inspection units in underground storage tanks (USTs). In 1998, all USTs in the United States were required to comply with strict environmental regulations (U.S. Army Corps of Engineers, 1999). Reliable assessment methods were needed to determine whether such tanks were in compliance. The Field Robotics Center at Carnegie Mellon University developed a mobile inspection robot for the Army Corps of Engineers (2001). The Neptune is designed to inspect both above ground and underground storage tanks for corrosion and visible deterioration. Magnetic tracks propel the robot and keep it in contact with the tank surface. An ultrasonic transducer mounted to the robot provides information about tank wall thickness. Neptune is completely sealed and can operate in full tanks. In highly viscous fluids, an acoustic positioning system is deployed for navigation.

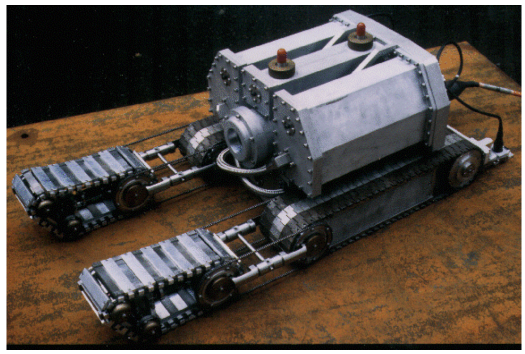

Figure 1-7. Neptune storage tank inspector (U.S. Army Corps of Engineers, 2001).

Robots and Safety

In addition to enhancing inspection capabilities and decreasing costs, robotic systems may also improve worker safety. Inspectors are exposed to numerous potential hazards while performing routine tasks (FHWA, 2002b). Inspecting bridges and other large structures usually requires inspectors to climb to various locations, often at great heights or above waterways. Confined spaces such as culverts and tanks may have inadequate ventilation, resulting in low oxygen levels or high concentrations of toxic or explosive gases. Any type of underwater inspection can always pose the threat of drowning. These potential threats could be reduced by deploying robots rather than humans to hazardous locations.

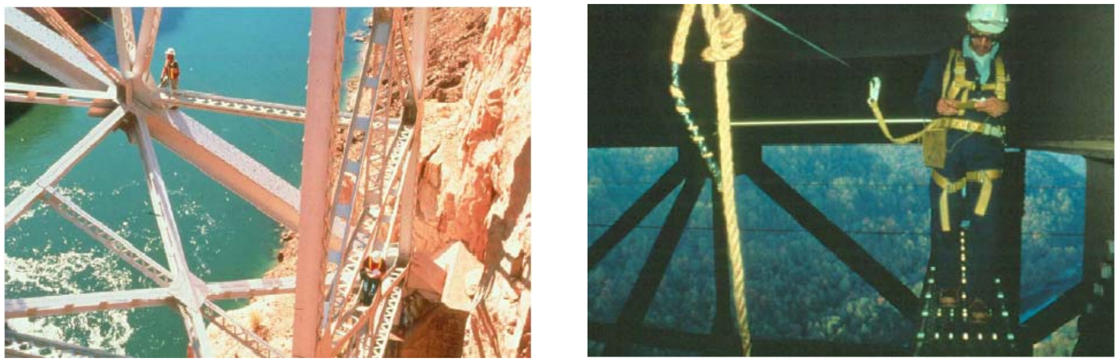

Figure 1-8. Routine inspections often require climbing (FHWA, 2002b).

The likelihood of an accident occurring in a hazardous location can be further increased by certain human attributes. Monotonous or repetitive tasks may result in boredom, causing an inspector to fall into an inattentive state. A worker may take shortcuts that sacrifice safety for time if he becomes overly confident in his capabilities. Performing tasks without incident may result in a false sense of security that leads to carelessness. There are numerous reasons why people make mistakes. Eliminating human error as a potential threat could greatly reduce the possibility of an accident occurring. Robots may cost money, but when compared with a human life, they are expendable.

Autonomous Systems

While many of the current robotic technologies provide improvements in inspection capabilities, few systems incorporate fully autonomous robots. Employing an autonomous robotic system becomes quite challenging when faced with the uniqueness in design of civil structures. A system that works on one structure may not work on another due to small or large design variations. An autonomous robotic inspection system must have the ability to adapt to environmental changes by using advanced sensor networks. This paper will describe in detail steps taken towards developing an autonomous robot inspector. Specifically, methods of creating a basic sensor network that can integrate various inspection devices will be included.

Chapter 2
Proof-of-Concept: A Robotic System for Structural Health Monitoring of Bridge Girders

2.1 Developing a Task Specific Robot

Autonomous Systems

A functional autonomous robot requires the addition of two components to its remote-control counterpart: an information processing system capable of interpreting input signals and sending control output signals to the various mobility constituents, and a peripheral sensor network that relays information to the processing system. These components can be simple or complex, however the autonomous system must have the ability to adapt or respond to environmental stimuli.

The complexity of an autonomous robot depends primarily on the number of tasks or functions it can perform in response to various stimuli. A simple robot may only perform one task, such as stopping when it encounters an object. A more complex robot may be able to stop when it reaches an obstacle and then use various sensors to correct its course and continue. While the maneuverability of a robot depends on the mechanical design, the ability to respond to different stimuli depends on the capabilities of the processing system.

An autonomous robotic inspection system has several advantages over current non-autonomous designs. While many of the developing technologies employ remote-control, semi-autonomous, and tele-operated techniques, which allow for enhanced accessibility as well as increased worker safety, there are still limiting factors to such systems. Remote control requires the presence of an operator, who must remain focused on the task as if he were performing the inspection without the assistance of a robot. Additionally, many remote-control systems are tethered by a power cable, a data transmission cable, or both. Thus the operating range becomes limited by the length of power cords. While even a simple remotely controlled tethered system provides significant improvements in inspection capabilities, the limited range of operation as well as the reliance upon an operator could be eliminated with an autonomous system. It should be noted, however, that wireless semi-autonomous robots require large-bandwidth, high-fidelity data transmission, which poses an additional set of technical, human interface, and energy-related challenges.

A further advantage of an autonomous system is the possibility for long-term deployment. Routine visual and advanced sub-surface inspection can be effective in preventing structural failure by identifying problematic conditions. However, continual measurement of certain physical parameters may also provide information about structural health. Strain, temperature, vibration, and displacement are all indicators of environmental conditions. A particularly harsh environment, which would affect such parameters, can certainly lead to premature structural failure. Additionally, different types of severe conditions may cause different types of deterioration. For example extreme temperature gradients may cause expansion cracks while high moisture levels may cause corrosion. An autonomous system deployed at a site for days, months, or even years could acquire data that would indicate long-term patterns of environmental conditions. Such information might be useful in determining the necessity for in-depth inspections, as well as identifying certain structural elements, which may be more susceptible to premature failure.

Embedded Sensor Networks

One method for enabling long-term structural health monitoring is to use embedded sensor networks. Fiber optics cables, strain gages, and various other sensors can be embedded within composite and concrete members during construction. Such sensor networks provide real-time and continuous measurements of physical parameters that affect structural health.

Figure 2-1. Embedded corrosion sensor (Fortner, 2003).

Figure 2-1 shows an embedded corrosion sensor developed by Virginia Technologies, Inc. of Charlottesville, Virginia (Fortner, 2003). The ECI-1 (Embedded Corrosion Instrument) contains a variety of sensors including a chloride threshold indicator, a conductivity and resistor sensor, and a temperature sensor. The ECI-1s are placed throughout a steel reinforcement structure before concrete is poured. The sensors are hardwired together to allow cross communication. Additionally, power and communications cables are connected to an external data collection unit. Once concrete is poured, information regarding subsurface conditions can be acquired from the data collection unit via a laptop computer.

While such embedded sensor networks allow access to valuable information, they are often impractical due to high costs. Sensor installation can be extremely labor intensive and expensive, often consuming close to 25% of the overall project budget (Taha et al., 2002). Data sampling is accomplished by connecting to these sensors through wires that protrude from within the structure. Management of these wires can account for increased installation time. Furthermore, supplying power to embedded sensors creates additional complications. Hardwired sensors are costly due to the increased labor of installation, while battery powered sensors are less reliable and require frequent maintenance. A further, and perhaps more fundamental, limitation of embedded sensors is that severe structural damage can often be extremely localized. Unless the sensor is embedded in proximity to the damaged location, it may not be able to sense the damage. For example, it is difficult to sense the presence of a crack, using an array of strain gages, unless the crack occurs at the location of one of the gages.

Many of the complications associated with embedded sensor networks could be eliminated with a system that employs Addressable Sensing Modules (ASMs). MicroStrain, Inc. of Williston, VT is currently developing programmable ASMs to sample data from embedded sensor nodes (Arms, 1999). These ASMs incorporate a telemetry system capable of transmitting data to a remote source, thus eliminating the need for lead wires. Dependence upon batteries and power cables is also unnecessary as the ASMs are capable of inductive powering. Reliability of the system is increased with the elimination of hardwiring as each sensor can function independently. Failure of one sensor will not have an impact on the performance of other sensors within the array. Furthermore, the ASMs are compatible with microelectromechanical systems-based (MEMS) sensors, such as accelerometers, inclinometers, and strain detectors that can be externally mounted to the structure. These sensors decrease labor costs, as their installation is relatively simple compared to the installation of embedded sensors. Additionally, the externally mounted sensors can be relocated, thus creating an adaptable sensor array.

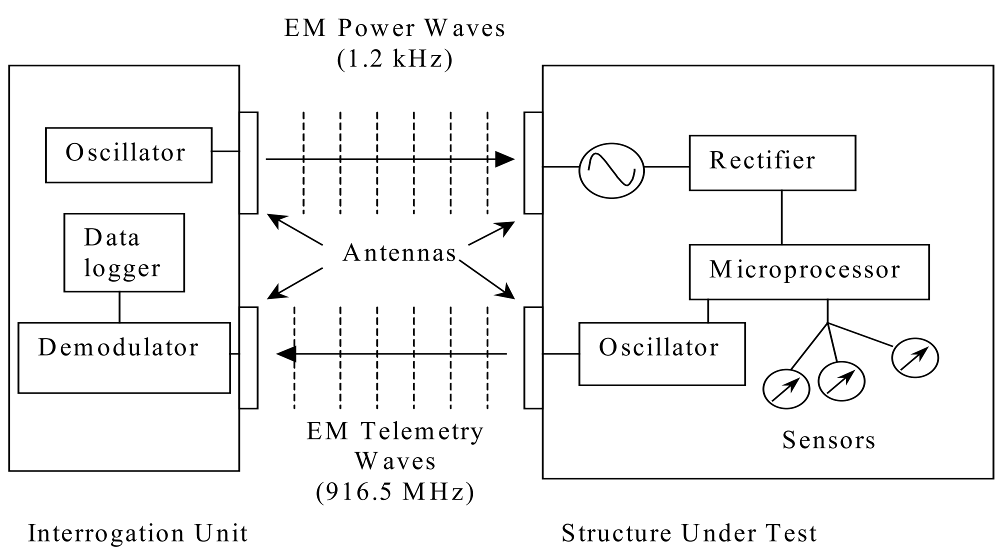

Figure 2-2. ASM block diagram.

The long-term deployment capabilities of autonomous robots make them a prime candidate for use with ASM systems. The concept of an autonomous inspection system providing continual surveillance could be realized with such integration. A mobile robotic platform, with the ability to move throughout a structure, could interrogate an array of ASMs. With a power amplifier converting DC power to AC power, the DC power supply of the robot could drive an on-board inductive powering coil that would generate an AC magnetic field. With the robot in close proximity to an ASM, the generated AC magnetic field could then induce an electric current in the ASM target coil, thus providing power to the sensor node. Additionally, a robot with data storage capabilities and a mounted transceiver could download information from the senor nodes. The reduced distance of transmitting to the robot versus a remote location would decrease the power necessary for operating the ASM telemetry system.

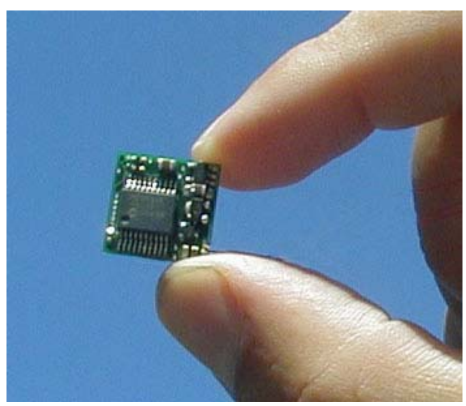

Figure 2-3. Wireless sensor node (MicroStrain, Inc.).

Thus, an autonomous robot compatible with an ASM system could provide frequent sensor interrogation. This would enable long-term deployment and continual surveillance of the structure.

Bridge Girder Inspection

Investigating the feasibility of developing an autonomous inspection system required a task that would allow the practical implementation of such a system. To achieve a plausible, yet successful proof-of-concept, creating a simple autonomous robot for the inspection of steel girders, typically employed on highway overpass bridges, was chosen as the target task.

Bridge girder inspection was a practical choice for several reasons. Bridge girders are relatively uniform in design. While variations in dimensions may exist from one structure to another, a concept that works for one bridge is likely to be widely applicable with only minor modifications. Bridge girders can be fracture critical members, meaning the failure of any such member can result in the catastrophic failure of the entire structure. Thus, advancements in inspection techniques for critical members have significant importance for structural health monitoring. Bridge girders are also extremely common, providing numerous opportunities for field deployment.

Another benefit of using bridge girders is the feasibility of incorporating an ASM system. The possibility of magnetically mounting sensors to a steel beam flange would create the opportunity for developing an autonomous system not only capable of short-term routine inspection, but also capable of long-term continual structural surveillance and interrogation of ASMs.

Design Constraints

After determining a task sufficient to prove the feasibility of the autonomous inspection system, the next step was to identify the design constraints of the project. These constraints included those imposed by the geometry of the structure as well as the limitations created by the payload (i.e., on-board inspection instruments or interrogation system).

Because I-beams are commonly used as bridge girders, the primary physical constraint was imposed by the geometry of such a beam. The objective required the robot to travel along the exposed beam flange and record measurements of either physical parameters or structural integrity. Thus, some of the physical constraints included a design that would allow the robot to be mounted on an I-beam flange, as well as a drive system that was capable of propelling the robot across the span of the beam while using the flange as the drive surface.

Additional physical constraints were imposed by the inspection capabilities required of the robot. The robot could be viewed as a mobile platform for transporting inspection devices or an interrogation system to various locations. Thus, the design of the robot needed to account for carrying such a payload by creating sufficient weight-carrying capability, platform space, and on-board power.

Aside from the physical constraints imposed on the design, certain intelligence capabilities were also required. The ability to stop at predetermined locations for inspection or interrogation created the need for a processing system that could interpret signals from a peripheral sensor network as well as control a drive system. Additionally, some capacity for data storage was needed—either as part of the processor memory or as a separate on-board system.

Finally, certain power restrictions were imposed by the objectives. The desire to eliminate the need for a tethered system required the robot to carry an on-board power supply. The power supply needed to be large enough to power the robot drive system as well as the processor and peripheral sensor network for the duration of at least one round trip (assuming the robot has a base station where the power supply can be recharged between inspection or interrogation trips). Additionally, the robot would have to power the sensor and/or payload. This could mean anything from an on-board video camera for visual inspection, to an inductively powered ASM telemetry system found in an embedded sensor node. In any case, such power requirements would be determined by the number of inspections or interrogations performed during each round trip.

2.2 Beam-Crawler Prototypes

Phase I

The first step in the fabrication process was to demonstrate that an autonomous system could work in the controlled environment of a laboratory. This process specifically entailed producing a mobile robotic platform capable of following a predetermined path, locating and inductively powering a remote sensor node, and collecting data.

To implement this plan, the low-cost LEGO Mindstorms® robotic system was used (Arms, 1999). A mobile platform driven by the LEGO® system was assembled using a photo sensor for optical tracking and multiple touch sensors for triggering motor control. A sensor node, consisting of a remotely powered Addressable Sensing Module (ASM) and five solid-state semiconductor temperature sensors, was mounted on a sheet of Plexiglas® and then inverted to simulate an embedded node. On the topside of the sheet, black electrical tape was laid out as a path for the robot to follow. The light-dark transition provided by the tape created enough contrast to enable optical tracking with the photo sensor. Small markers were placed over the embedded node to trigger the touch sensor motor control.

Figure 2-4. Phase I robot with photo sensor and inductive power coil.

The robot towed a trailer carrying the power supply and excitation hardware. The remote powering coil was mounted to the anterior of the robot. The robot performed numerous test runs where it would navigate the taped path and stop at the embedded sensor node. The markers triggering the cessation of movement were placed to achieve alignment within 10mm of concentricity between the powering coil of the robot and the

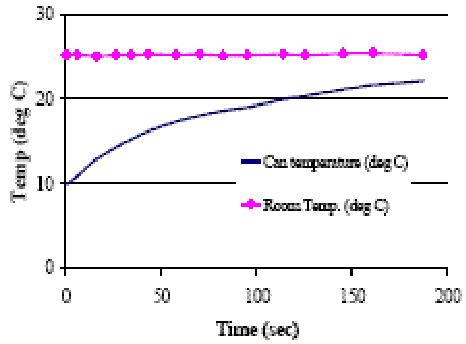

Figure 2-5. Typical data acquired by Phase I robot.

power reception coil of the node (Arms, 1999). The following 2-3 minute duration of rest time allowed the robot to power the ASM, which then transmitted temperature data to a remote radio frequency receiver and computer.

The robot successfully navigated its course, located the ASM and powered it to enable remote data acquisition with no human control or intervention (Arms, 1999). Thus, the feasibility of a simple autonomous system had been proven.

Phase II

The next phase of development involved implementing a more practical design. The previous design successfully accomplished the inspection task about a simple two-dimensional geometry, which imposed few physical constraints. A more sophisticated design, which could perform a task that better simulated the more complex bridge girder inspection, was desired.

A laboratory I-beam was chosen for testing. The geometry of the beam was similar to that of a bridge girder, yet the laboratory provided a controlled environment to facilitate debugging. The chosen design consisted of a hanging aluminum U-frame, suspended from the bottom I-beam flange by four wheels. The 64mm diameter wheels, equipped with rubber tires, provided the robot with both suspension and propulsion. A 2-wheel drive system was established by the use of a DC motor and a series of gears which synchronized the two drive wheels. An electronic speed control and a 7.2V rechargeable battery pack supplied the motor with power and control.

Figure 2-6. Phase II robot.

Control of the entire system was provided by a Z-World Jackrabbit BL1800 microcontroller and a network of touch sensors similar to those used in Phase I. The overall concept of deployment was similar to that of Phase I as well. The predetermined path was defined by the restrictive geometry of the beam, while the embedded ASM nodes would again trigger the cessation of the robot movement via the touch sensors. A more detailed analysis of the electronics and the microcontroller capabilities will be provided in the upcoming discussion of the field test model.

The greatest difference in the design concept of Phase II versus Phase I was the on-board data storage capability provided by the Jackrabbit microcontroller. While the Phase I model triggered data transmission to a remote station, the Phase II robot could receive and store data in the Jackrabbit's memory (Esser et al., 2000). The on-board storage capability greatly decreased the necessary transmitting distance. Instead of requiring the ASM telemetry system to transmit from the node to a remote station, data could be directly transmitted to an on-board receiver located only centimeters from the node. Transmitting over a shorter range dramatically decreased the power necessary for the ASM operation, which in turn effectively improved the power efficiency of the robot, allowing it travel greater distances before recharging (Esser et al., 2000). After data acquisition was achieved, a telemetry system linked to the Jackrabbit memory could transmit stored data to a networked computer located at the robot base station. Once uploaded, data could then be accessed immediately via the Internet.

Several laboratory tests were conducted to evaluate the performance of the robot. The ASM system was linked to a strain gage that was mounted on the beam. The robot was able to successfully locate the sensor and retrieve strain data while the beam was loaded (Huston et al., 2003). Figure 2-7, shows a data sample collected by the robot.

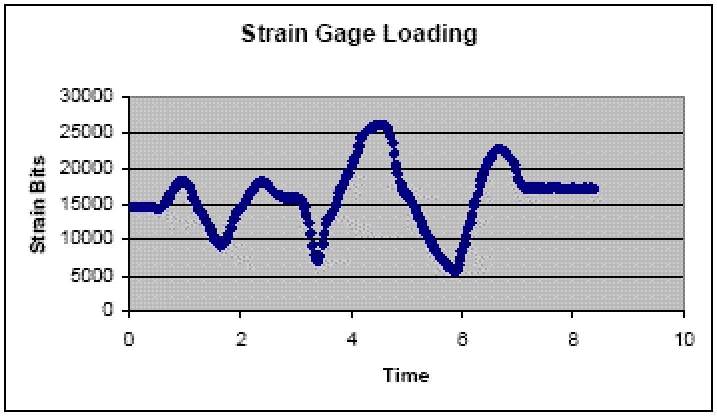

Figure 2-7. Strain data acquired by Phase II robot.

Thus, the early phase development of the "beam-crawler" was a progression from a simplistic proof-of-concept model to a more practical and complex design. The Phase I model provided proof that it was feasible to use low-cost, off-the-shelf components in building an autonomous robot capable of locating and powering an ASM. The Phase II model demonstrated the sophisticated design necessary for accomplishing the same task in a more complex and realistic environment. After achieving success with the laboratory deployed beam-crawler, the project was ready for field implementation.

Chapter 3
Field Implementation of the Autonomous Beam-Crawler

3.1 Field Specific Requirements

Objectives

The first step in the field implementation of the beam-crawler was to choose a structure for deployment. The LaPlatte River Bridge on US Rte. 7 in Shelburne, VT was chosen for its convenient location. Additionally, the recent construction of this bridge suggested that its geometry was representative of current designs.

The primary task was to develop a mobile robotic platform for carrying and using sensing and interrogating systems to monitor the structural health of the bridge girders. Additional objectives required the robot operate with minimal reliance upon manual control. While the project could be described as a proof-of-concept, the implementation in the field, rather than in a laboratory environment, elucidated design constraints specific to the chosen structure as well as generic issues related to robotic wireless inspection of structures.

Design Specifications and Constraints

Similar to the design requirements for the laboratory-deployed beam-crawler, the criteria for designing a field-deployed robot included the following: a drive train capable of moving along an I-beam bridge girder, a programmable control system to control the vehicle speed and direction, a peripheral sensor network to relay information to the controller, and a robust chassis capable of carrying a payload and a power supply. However, certain constraints imposed by the field structure necessitated design modifications of the laboratory robot.

The primary design constraint for the field-deployed beam-crawler was the girder geometry of the LaPlatte River Bridge. For the previous generation of beam-crawler, the simple beam geometry used in the laboratory permitted the use of large diameter wheels resting on the top surface of the flange to propel as well as support the robot. In field practice, however, geometry restrictions created the need for a modification of the drive system.

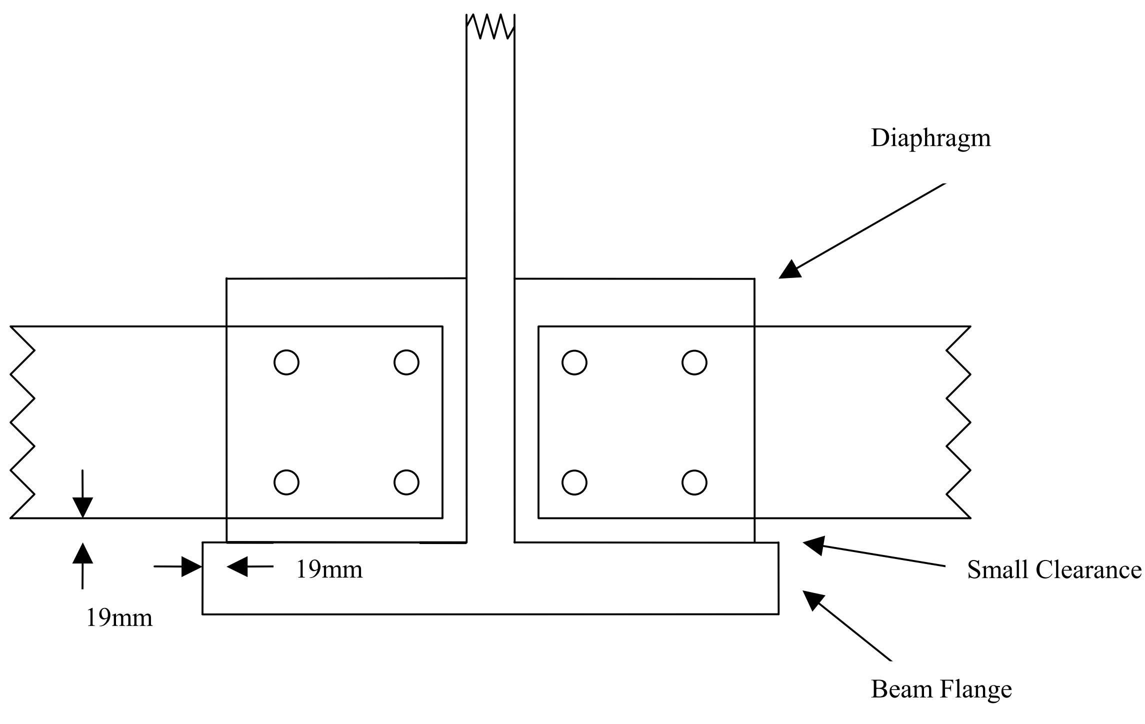

Figure 3-1. Beam Geometry of the LaPlatte River Bridge.

The placement of diaphragms at approximately 6-meter intervals created a difficult geometric design constraint. This particular diaphragm-to-girder attachment detail is an attempt to reduce the likelihood of fatigue crack formation in the girders. These diaphragms are fastened to the beam in a manner that leaves 19mm x 19mm clearance on the top surface of the flange, thus making the use of drive wheels on the top surface impractical due to the small size necessary for clearance.

Additional design constraints included the size and weight of the robot, as well as the intended duration of operation. The chassis needed to be large enough to carry a drive train, controller, sensors, and payload. However, a large and bulky design would create a heavier vehicle and would result in the need for a more powerful drive train and ultimately a larger power supply. While the objectives implied a minimal operation time corresponding to one round-trip across the beam, the desire to maximize the utility of the robot for potential future applications meant that minimizing power consumption was a key factor in the design. Aesthetics was also an important factor in the design. The robot needed to appear as a semi-finished product with no loose wires or other inappropriately exposed components that would detract from the overall visual appeal of the design.

3.2 Design and Fabrication

Once the specifications were established, design and fabrication of the current generation robot began. This section describes the design of the current generation, which can be simplified into three basic components: the chassis, the drive train, and the electronics or “brains”.

Chassis

The chassis is an open-ended plywood box, roughly 0.50m x 0.60m x 0.24m, which provides a platform for mounting the drive train and the electronics. Plywood was chosen for durability, low cost, and ease of fabrication. Mounting the chassis to the beam presented one of the most challenging obstacles to the design. The mounting mechanism needed to be capable of carrying the substantial load of the robot and payload, yet small enough to clear the diaphragms. Several possible mechanisms were considered, including a set of V-groove wheels that could rest on the corners of the flange at a 45 degree angle. However, even the smallest off-the-shelf models of V-groove wheels could not provide the necessary clearance. Ultimately miniature roller bearings designed with thrust-load bearing capability were selected and successfully used.

These 16mm roller bearings are incorporated in a set of four separate roller units that are fastened to the interior four corners of the box. Each roller unit consists of bearings mounted on shoulder screws to an aluminum block. The shank of each screw provides an axle for the bearings. The rollers enable low friction mounting to the beam flange by utilizing two sets of the 16mm bearings on top of the flange to allow for the approximate 19mm x 19mm clearance needed for the diaphragms. Originally, an additional set of bearings was used underneath the flange to act as a vertical guide. However, this set was removed after initial testing indicated it was unnecessary.

The chassis is wide enough so that 3mm clearance exists between the sides of the flange and the chassis. Delrin™ blocks are fastened to each roller unit to provide low friction guidance along both edges of the beam flange and to counteract any steering or directional misalignment. Each unit is fastened to the chassis by three socket screws. The chassis can be quickly mounted to the beam by removing the socket screws of two roller units from one side and refastening once the chassis is in place. One person can accomplish mounting and dismounting in typically fewer than five minutes. Because mounting and dismounting increases thread wear, heli-coil inserts are used in the aluminum threads to prevent premature thread stripping.

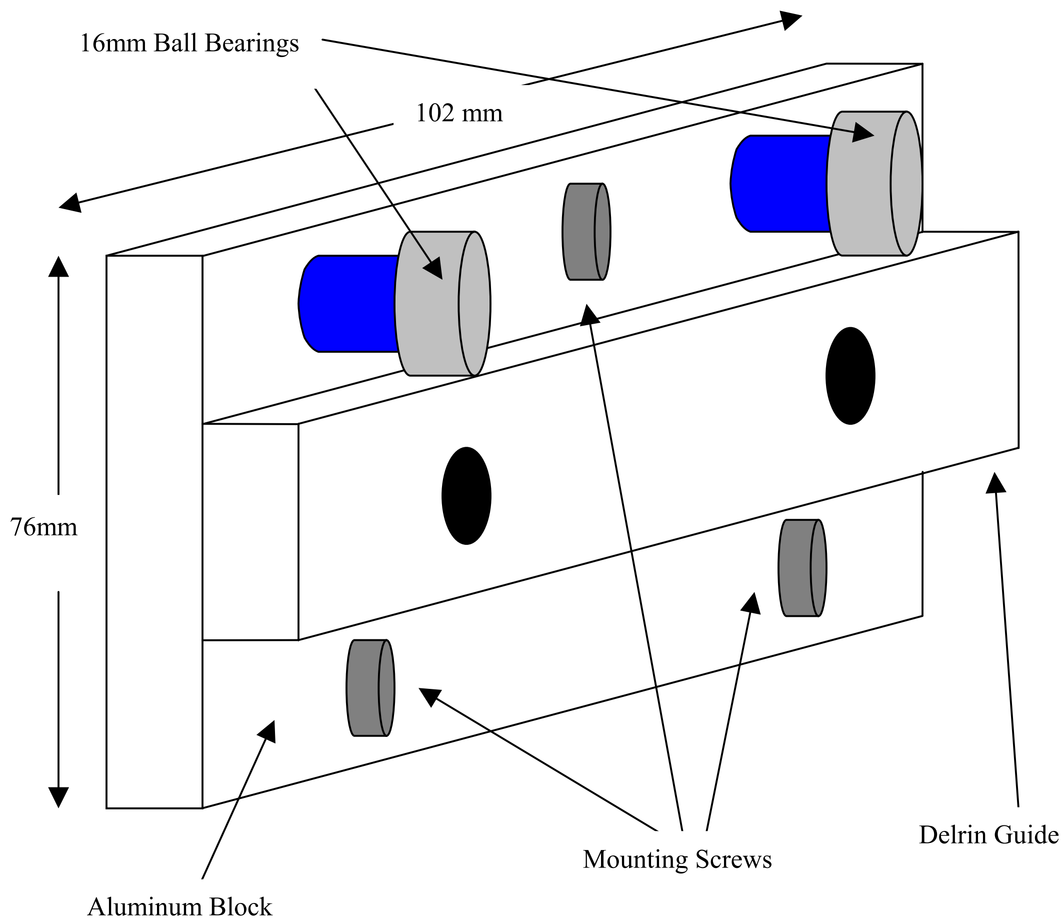

Figure 3-2. Roller unit.

Drive Train

The drive train for the robot is a modified high-end (approximately \$350) radio controlled hobby truck (Traxxas® E-Maxx™). Mounting the drive train inside the box upside down allows the drive wheels to contact the bottom of the flange. Pressure on the drive wheels is needed to create sufficient tire traction so that slipping does not occur. Because the bottom of the flange is used as the drive surface, but the weight of the robot is suspended from the top surface, a fair amount of traction is required. Traction pressure is supplied by the built-in, large-travel suspension of the truck chassis. When the robot is mounted on a beam, these springs are compressed to supply enough force to the drive

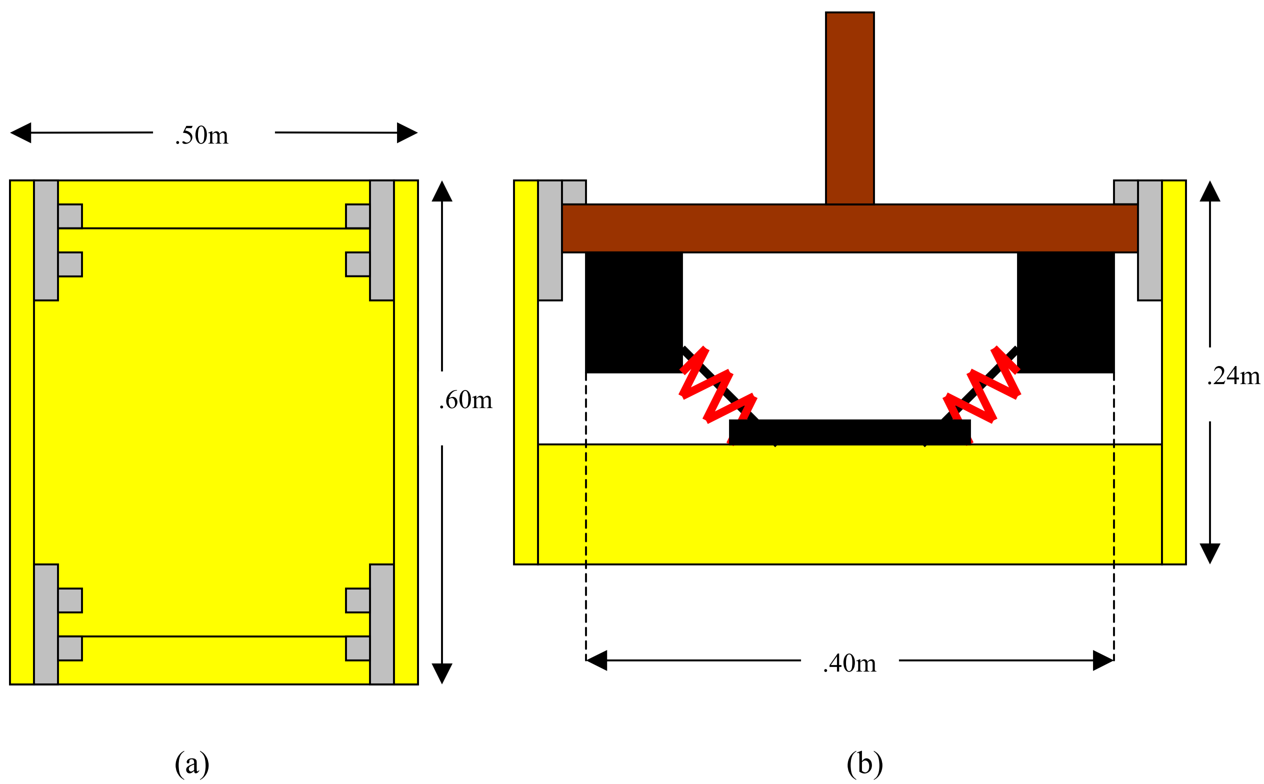

Figure 3-3. (a) Overhead of chassis. (b) Chassis and mounted drive train on beam.

surface to create good tire traction. Dual motors apply ample torque to the drive shaft of the four-wheel drive system so as to enable starting on a small incline.

Most of the modifications made to the truck involved the removal of various superfluous plastic parts. These parts include the body, bumpers, skid plates, and various unused mounts. Additionally, some modifications were made to the transmission. Because the beam crawler operates at low speeds, the gearing was changed by replacing the two 18-tooth pinion gears with 12-tooth gears. Thus, with the 66-tooth spur gear, the gear ratio was reduced from 3:11 to 2:11.

Electronics

The "brains" of the robot consist primarily of a Z-World Jackrabbit BL1810 programmable microcontroller and three photo-sensors. The Jackrabbit is programmed using a PC and Dynamic C® software. The photo-sensors are connected to various digital input ports on the Jackrabbit. Several off-the-shelf sensors were considered before the decision was made to use custom built sensors due to their low cost and relatively simple design.

Each photo-sensor consists of a white LED and a photo-resistor mounted opposite to each other. The LED is connected to a 5 V power supply and emits light towards the photo-resistor, which is connected to a digital input port on the Jackrabbit. The photo-resistors have a nominal 20MOhm dark resistance and a 50kOhm light resistance. The sensors communicate with the controller through the use of transistor-transistor logic (TTL). Although the photo-resistors send an analog voltage signal to the digital ports, a large enough change in resistance will act as a high/low input to the controller. Thus the Jackrabbit will read a large change in light exposure to the sensor as a logic signal. The photo sensors will normally put out a TTL-level high signal of 4.6 V. If an object comes between the LED and the resistor, thus blocking the light to the resistor, the sensor will send a TTL-level low signal of 0.1 V.

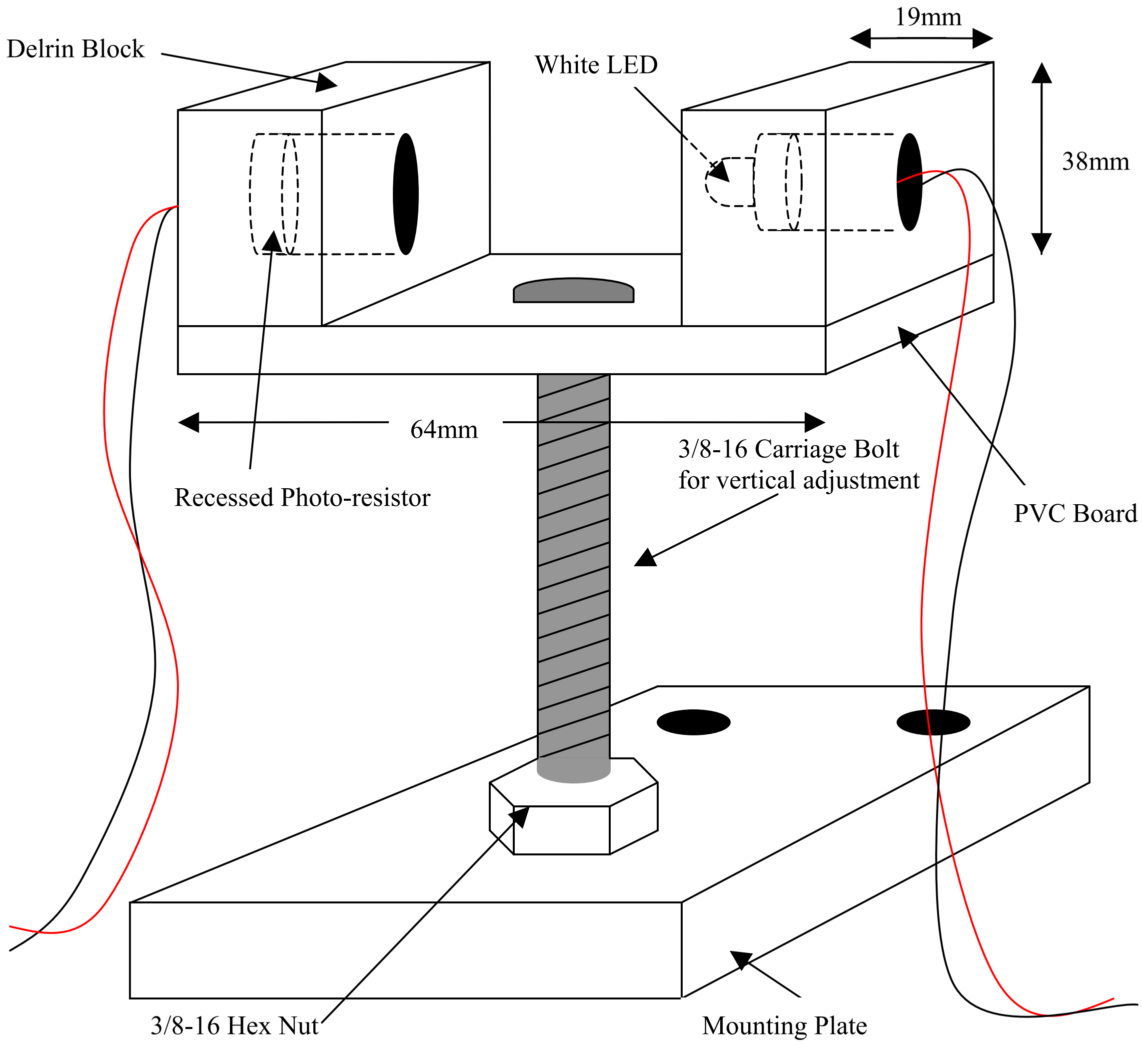

Figure 3-4. Photo-sensor.

Mounts for the photo resistors and LEDs were initially machined from white Delrin^{TM}. The photo-resistors were recessed in the plastic blocks. Testing indicated that the light color of the plastic had a significant effect on the resistance. Even when the direct light path of the LED was blocked, the white plastic reflected enough ambient light to cause insufficient resistance. Instead, using black plastic dramatically decreased the amount of light exposure to the resistor.

Additionally, several types of photo-resistor were tested. It was found that while resistors with a smaller light/dark resistance range were sufficient to provide a logic signal, the smaller range in resistance did result in a delay in the high/low output response. The resistors needed to be sensitive enough so that a small object moving at the robot's speed through the light path would elicit a high/low response. The current 20Mohm/50kohm resistors are sensitive enough to respond to small objects (~10mm long) even when the robot is moving at high speeds.

The drive train of the robot also has electronic components in the control and power systems. These include a 27MHz transmitter and receiver, transmission and steering servo motors, and an electronic speed controller (ESC). The receiver has three channels that send varying 5 V pulse width modulation (PWM) signals at a frequency of about 500Hz to the two servos and the ESC. The pulse width of these signals is determined by the transmitter. The transmission signal has one of two discrete pulse widths that correspond to one of two servo arm positions. A 0.5ms pulse width will engage low gear and a 1.0ms pulse width engages high gear. The steering signal has a range of pulse widths, which allow for small steering adjustments. A 0.6ms pulse width corresponds to a full left position of the tires, 0.9ms corresponds to a neutral wheel position, and a 1.2ms pulse corresponds to a full right position.

The ESC is connected to two 6 cell (7.2 V) 1500 milliamp-hour NiCd rechargeable battery packs. The ESC supplies power to the dual motors, and, by means of a battery eliminating circuitry, to the receiver as well. Similar to the inputs to the steering servo, the input signal from the receiver to the ESC has a range of pulse widths. The ESC regulates the motor speed and direction by varying the current supplied to the motors. The pulse width of the ESC input signal determines the ESC current output. Thus the pulse width ultimately controls the motor speed and direction. A pulse of 1.2ms corresponds to full forward, 0.85ms corresponds to neutral, and 0.6ms corresponds to full reverse. Additionally, the ESC employs smart braking, where the circuitry reduces vehicle speed before engaging reverse.

The Jackrabbit controller can be programmed to send a 5 V PWM signal from a digital output port. This signal can be modified to match the frequency and pulse width of the receiver's signal to the ESC. Thus, connecting the ESC to the Jackrabbit instead of the receiver creates the possibility for autonomous operation. However, this situation results in a purely autonomous mode with no possibility for remote manual control. In order to achieve two possible modes of operation, the Jackrabbit, the receiver and the ESC are connected to a relay switch. With no power supplied to the relay, the ESC will receive the signal from the receiver, thus enabling manual remote operation. However, if power is supplied to the relay, the ESC will receive the signal from the Jackrabbit and will thus operate autonomously.

The transition from manual to autonomous mode and vice versa can be triggered remotely by using the transmitter. Because the beam-crawler has no need for the shifting servo (the drive train only needs to operate in low gear for beam crawling), the shifting servo arm was detached from the transmission and is now used as a lever to operate a mechanical switch, which connects a 5V power supply to the relay switch. Using the shifter control on the RC transmitter will open or close the switch and thus trigger the relay to send either the receiver signal (manual mode) or the Jackrabbit signal (autonomous mode) to the ESC.

The use of these various electronic components led to the need for multiple power supplies. The Jackrabbit operates on 9-25VDC. The relay, the receiver, and the LED's all use 5VDC. Because the receiver is no longer connected to the ESC, it needs another supply. Additionally the ESC operates on 14.4VDC. Initially, separate battery packs were used for each different component. However, this created a bulky system with multiple sources for potential power failure. Several options were considered for consolidation. Currently, a 12V motorcycle battery is used as the main power supply. The 12V battery is connected directly to the Jackrabbit, while a circuit board with a 5V regulator powers the LEDs and the relay. The receiver was also connected to the circuit board, however due to the large current draw of 1.5A by the receiver, the voltage regulator could not supply enough current to the other components. Instead, the receiver was equipped with a separate 6V battery pack power supply. Attempts were also made to power the ESC with the 12V battery. However, the ESC is limited to operating only on 14.4V, so the two 6 cell battery packs remain as the power supply for the ESC.

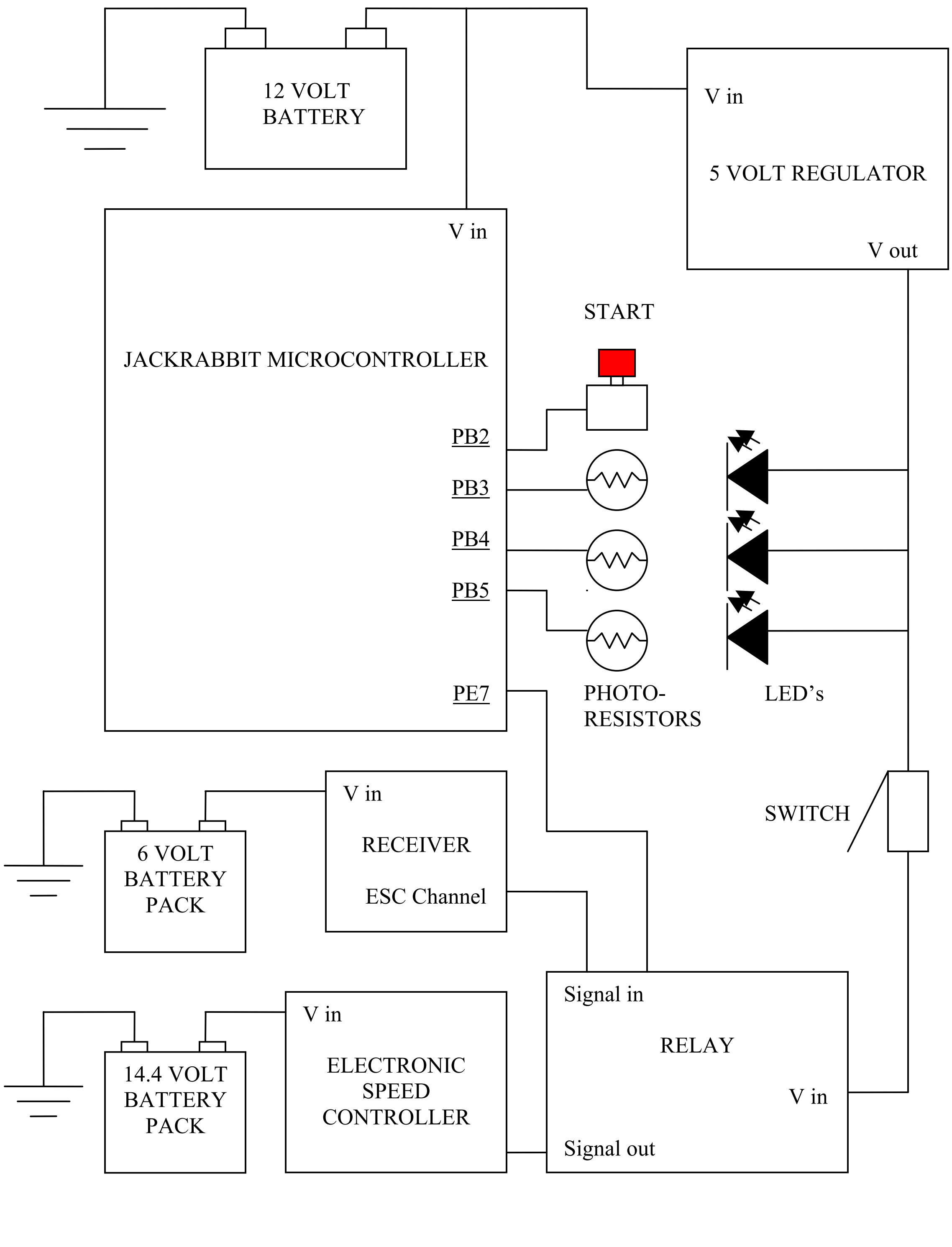

Figure 3-5. Robot electronic system block diagram.

Table 3-1. Electronic component power requirements.

Component	Voltage (V)	Current (mA)	Operating Power (milliWatts)
Drive System* (Motors, Receiver, Servos, etc.)	14.4	10,600†	153,000
Jackrabbit	12.0	500	6,000
Relay	5.0	120	600
Photo Sensors (3)	5.0	60	300

* Drive system includes receiver operating with battery eliminating circuitry
† Calculations based on endurance test described in Section 3.4

From Table 3-1, it is apparent that the drive system uses significantly more power than any other electronic component. Thus, the duration of operation is limited by the capacity of the power supply for this system.

3.3 Programming

As the robot operates autonomously, the Jackrabbit controls the motor speed and direction. Using Dynamic C® software, the Jackrabbit is programmed to send varying PWM signals from a digital output port to the ESC. The program changes pulse width by varying the duty cycle, which is represented by an integer between 0 and 100. The duty cycle for a neutral motor signal lies between 59 and 63. In order to achieve minimum speed in both forward and reverse, a pulse width barely greater and barely less than the neutral pulse width is used for slow forward and slow reverse, respectively. Thus, using the smallest increments, the low speed forward duty cycle is 64 while the low speed reverse duty cycle is 58. The program uses signals from four different digital input ports to change the duty cycle of the motor control signal. As described earlier, the photo-sensors are connected to three of these input ports. The fourth port is connected to a start button, which begins the program when pressed.

Once started, the Jackrabbit will send a low speed forward signal to the ESC until one of the sensors triggers a reverse signal for 0.5 seconds, a neutral signal for 5 seconds and then resumes the forward signal. Using the smart braking, the short duration of the reverse signal acts as a brake before the neutral signal, thus reducing the amount of distance required for the robot to stop. A second sensor triggers a low speed reverse signal until the third sensor triggers a neutral signal that lasts until the program is restarted. Each sensor can be triggered by blocking the light from the LED with small objects placed at various locations on the beam. Thus, the first sensor stops the robot at predetermined locations for data collection. The second sensor starts the return trip at a destined end location, and the third sensor stops the robot when it returns "home".

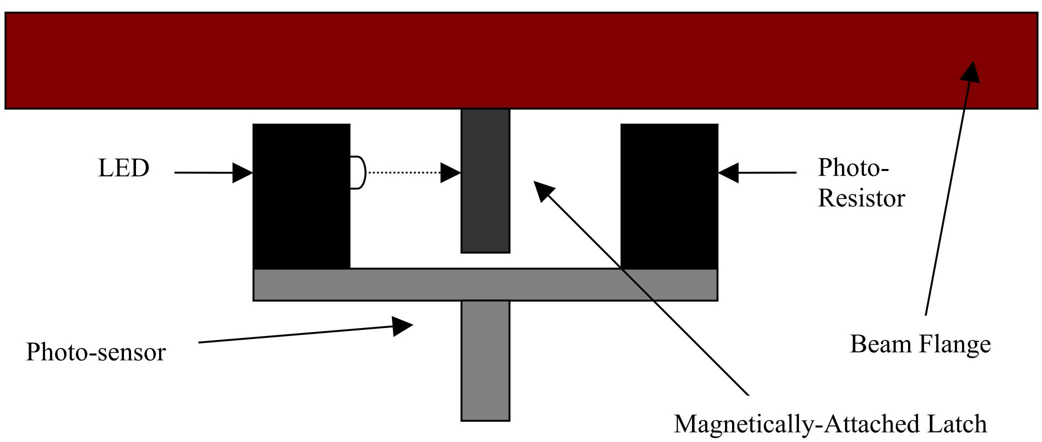

Figure 3-6. Magnetic latches placed on the flange break the light path between the LED and the resistor.

3.4 Field Tests

Performance

Several field tests have been performed. Numerous trial runs were also conducted in the lab prior to on-site testing. The first test verified the feasibility of the chassis design. The robot chassis was mounted to the beam flange and rolled across a span of about 15 meters. The chassis was able to clear the diaphragms and roll smoothly. The frame was sufficiently robust to support the hanging body weight of a person. Thus, no additional design modifications were indicated.

The second field test used a low end RC truck as the drive train. That model initially had difficulty moving up small pitches in the beam, so the large rubber tires were replaced by foam wrapped with grip tape to give the wheels a smaller diameter and more

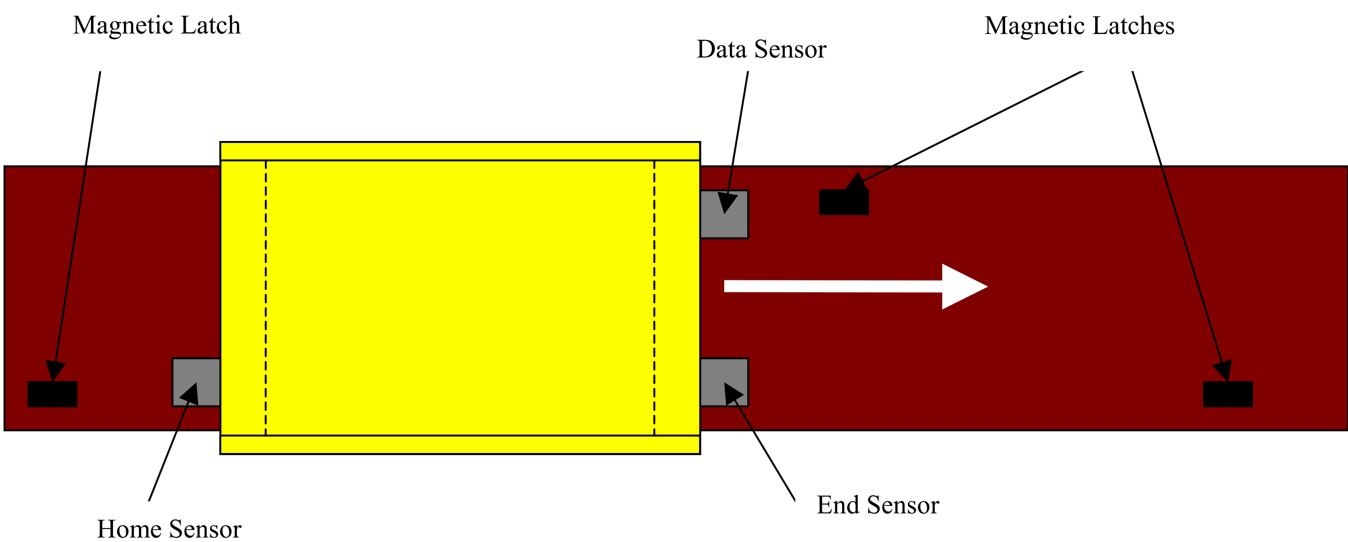

Figure 3-7. Placement of magnets for sensor triggering. When triggered, the data sensor will stop the robot for 5 seconds, the end sensor will reverse the robot direction, and the home sensor will stop the robot until the program is restarted.

torque. The modification improved the ability of the robot to ascend slight pitches. However, starting on an incline still proved difficult. This problem was solved by using a more powerful high-end RC truck. The high-end truck drive train allowed the robot to traverse the bridge girder at both high and low speeds. There was no difficulty in starting up a slight incline.

More recently, the robot was tested for its ability to operate autonomously. Magnetic door latches were placed on the beam to act as triggers for the photo-sensors. The robot successfully traversed the beam by stopping at each magnet for 5 seconds before reaching the last magnet and returning.

As a means for remote visual inspection and surveillance, a small wireless video camera was mounted to the robot chassis. The camera was aimed at the bottom of the

(a) (b)

Figure 3-8. (a) Latch passing through sensor. (b) Robot on return trip.

flange to closely photograph and record areas of interest that may otherwise have been difficult to access. The camera receiver was connected to a portable laptop computer.

Thus, immediate on-site information was attainable.   Figure 3-9 shows the camera and a typical image showing a dent on the girder.

(a) (b)

Figure 3-9. (a) Camera mounted on chassis. (b) Image from mounted camera that shows a dent on the girder.

Endurance

In addition to testing the performance capabilities of the robot, a test that demonstrated the maximum operation range was also performed. Due to the large capacity of the motorcycle battery (18Ah) and the relatively small current draw of the Jackrabbit, the relay, and the photo-sensors, it was believed that the drive system was the limiting factor in the endurance capabilities.

The robot was deployed on the bridge after the 3000mAh capacity batteries of the drive system were fully charged. It then repeatedly traveled at low speed across a section of beam spanning about 6 meters, making for a round trip distance of approximately 12 meters. The robot completed round trips continuously until its power supply was drained. In order to test the capacity of the drive system only, the Jackrabbit, sensors, and relay were not used. The robot was able to accomplish 64 round trips for a total distance of about 770 meters before low batteries affected performance.

The test was completed in roughly 17 minutes. Thus, a good approximation of the power consumed could be made:

$$\left(\frac{3000mAh}{17\min}\right)\times\left(\frac{60\min}{1h}\right)\times 14.4V = 152{,}470mW$$

This gives a general estimate for the power requirements necessary for deploying such a system. While the 3000mAh batteries allow for about 20 minutes of operation time before recharging becomes necessary, this time could be greatly extended by minor modifications to the drive system. The current electronic speed control (ESC) is only compatible with two 6-cell battery packs and thus cannot operate with a large 12V motorcycle battery. However, several ESCs exist that are compatible with a range of 4-10 cells. It would be feasible to incorporate one of these speed controls into the drive system, thereby enabling the entire electronic system to operate on a single 12V battery.

Using the operating currents from Table 3-1, an estimate can be made of the improved operating time if the entire system can run on one 18Ah 12V battery:

$$\left(\frac{18Ah}{11.28A}\right)\times\left(\frac{60\min}{1h}\right)\approx 96\min$$

Thus, the endurance of the robot could be greatly enhanced by modifying the drive system to accept a larger capacity power supply.

Results

The various design constraints specific to the LaPlatte River Bridge created the need for modification of the Phase II beam-crawler. Once a design was implemented, laboratory and field tests at various stages of development enabled debugging and further modification until a working field-deployable robot was achieved.

Results from field tests indicated that the robot had the ability to successfully operate autonomously for data collection. While mounting a video camera to the beam crawler and recording images demonstrated some basic inspection capabilities of the system, completion of a slightly more sophisticated inspection task was desired. Successfully integrating a sub-surface inspection device would prove the plausibility of the beam-crawler as an advanced inspection system.

Chapter 4
Beam-Crawler Applications: The Articulated Ultrasound Robot Arm

4.1 Ultrasound Inspection

Ultrasonic measurement was chosen as a sub-surface inspection technique for integration with the beam-crawler. The availability of an ultrasonic system and the widespread use of such instruments in structural health monitoring made ultrasound a logical choice.

Nondestructive Testing Principles

Ultrasonic testing is a practical method of nondestructive evaluation because it can be applied to a variety of materials (FHWA, 2002b). It is a non-invasive means of obtaining information about the sub-surface characteristics of a structural element. Ultrasonic testing has two primary inspection applications: thickness gauging and sub-surface flaw characterization.

Thickness gauging is crucial for pipelines, tanks, and other high-pressure containment systems. The wall thickness of such structures is a good indicator of overall structural integrity. Often, accurate thickness measurements are difficult to obtain due to the inaccessibility of the interior and sometimes the exterior of pipelines and storage tanks. Additionally, wall thickness may not be uniform throughout a structure, as deterioration from corrosion can often be localized. Thus, numerous samples are required for a true assessment. Ultrasonic testing is useful for thickness gauging because accurate measurements can be obtained with access to only one surface. Furthermore, the immediate feedback provided by portable ultrasonic gages enables multiple measurements to be achieved in a short period of time.

While larger structural members are not prone to thickness deterioration, the integrity of such members can be affected by the prevalence of sub-surface irregularities (FHWA, 2002b). Small cracks or inherent material flaws will escape visual detection. However, sensitive ultrasonic measurements can provide accurate information about the size and location of such irregularities.

Ultrasonic Theory

Sound waves are generated by mechanical vibrations transmitted through an elastic medium. Ultrasound refers to those vibrations occurring at a frequency above the human hearing range—generally greater than 20 KHz. Ultrasound waves behave similarly to sound waves. However, ultrasound waves are reflected off much smaller surfaces because of the short wavelength of the high frequency signals (GE Panametrics, 2003). This property is the basis for ultrasonic non-destructive testing.

The acoustic properties of a material can be described by the acoustic impedance and sound attenuation characteristics of the material. Acoustic impedance is the opposition to the sound wave generated displacement of particles within the material. Impedance has the following relationship to material density and sound velocity (GE Panametrics, 2003):

Equation 4.1 $Z = \rho c$

Z = Acoustic impedance
ρ = Material density
c = Material sound velocity

When a sound wave encounters a boundary between two media with different acoustic impedances, some of the sound energy is reflected off the boundary and some is transmitted through the new medium. The decibel (dB) loss of energy in the transmitted signal can be defined as (GE Panametrics, 2003):

Equation 4.2 $\text{dB loss} = 10\log_{10} [4Z_1Z_2/ (Z_1+Z_2)^2]$

Z_1 = Acoustic impedance of the first medium
Z_2 = Acoustic impedance of the second medium

Similarly, the dB loss of energy of the reflected, or echo signal is defined as (GE Panametrics, 2003):

Equation 4.3 $\text{dB loss} = 10\log_{10} [(Z_1-Z_2)^2/ (Z_1+Z_2)^2]$

Thus, a large change in acoustic impedance will result in a strong echo signal, while a small change in impedance will result in a very weak reflection. Additionally, if the impedance of the second medium is greater than the impedance of the first medium, the waveform of the echo signal will be inverted (GE Panametrics, 2003).

Mismatched impedance can apply to small discontinuities within a material. Low frequency sound waves may not reflect off small medium changes, but high frequency ultrasound waves with short wavelengths can be reflected from very small medium discontinuities. Thus, measurement of reflected ultrasound signals can provide information about structural integrity. For example, an ultrasonic excitation pulse applied to one side of a steel beam will travel through the specimen until it encounters the opposite side. The large impedance mismatch between steel and air will result in a strong backwall echo signal, which will travel back through the specimen. The thickness of the beam can then be measured as (Fowler et al., 2003):

Equation 4.4 $$T = c\Delta t/2$$

T = Thickness of the beam
c = Sound velocity in steel
Δt = Time measured between transmission of excitation pulse and reception of echo pulse

If the transmitted signal encounters a small flaw in the beam before reaching the other side, the mismatched impedance of the flaw will result in another reflection. Thus, any reflected signal that appears before a backwall echo is indicative of subsurface discontinuities or flaws.

In addition to the energy loss due to an interface, the acoustic energy of a signal will also diminish as the wave propagates through any medium. Different materials have vastly different attenuating properties. Energy loss occurs in cast metals and composites through scattering from individual crystallites in the casting or from boundaries of different materials within the composite (Fowler et al., 2003). Additionally, porous materials such as concrete have a similar scattering effect (Becker et al., 2003). The behavior of ultrasonic wave propagation in cement-based materials can be rather complex due to scattering caused by the randomly distributed aggregate. It is difficult to distinguish the attenuation caused by dissipation effects from that caused by scattering losses. Using diffusion theory, however, successful attempts have been made to quantify attenuation due to material losses (i.e. dissipation effects) from attenuation due to scattering losses (Becker et al., 2003). Thus, transducer sensitivity should be considered when testing materials with inherent discontinuities. If the transducer is too sensitive, it may be difficult to distinguish between flaws and material discontinuities. Attenuation occurs in low-density rubbers and plastics from absorption (Fowler et al., 2003). Thickness gauging of such materials is usually limited by this attenuation.

For testing purposes, ultrasonic signals are introduced to a specimen by means of a transducer, which transforms electrical energy into mechanical energy and vice versa. Because air is highly attenuating, the transducer is coupled to the test piece by water, a viscous medium, or a low impedance polymer (Fowler et al., 2003). The main components of a transducer are the active element, the backing, and the wear plate. Figure 4-1 is a diagram of a typical ultrasonic transducer.

The active element is usually a piezoelectric crystal that converts an electrical excitation pulse into an ultrasonic signal. The active element is interposed between the backing and the wear plate. While the active element will transmit a signal in both directions along the axis of longitudinal vibration, it is generally desired to have the signal propagate only in the direction of the test specimen. A signal transmitted from the back face of the active element will reflect off the back wall of the transducer and will thus interfere with the initial excitation pulse by increasing the duration of the waveform (GE Panametrics, 2003).

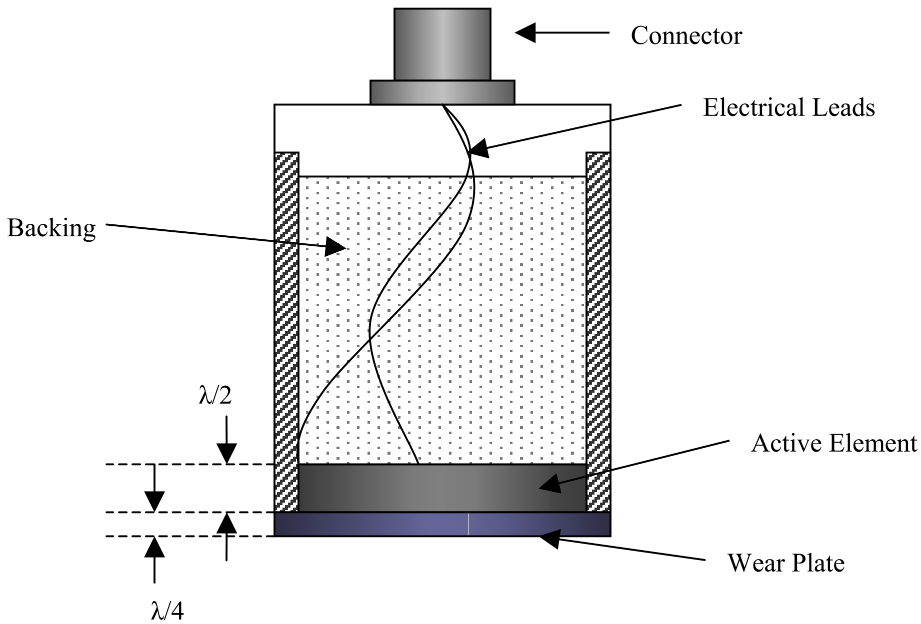

Figure 4-1. Ultrasonic transducer.

The transducer backing is used to minimize the transmitted signal waveform. A highly attenuating backing can be used to damp the vibrations of the element. Furthermore, if the impedance of the backing is close to the impedance of the element, the energy of the back face echo will also be minimized (GE Panametrics, 2003).

The wear plate is designed to protect the transducer element from the testing environment. Because transducers are generally used in direct contact with a specimen, the wear plate must be durable and corrosion resistant. The thickness of the wear plate is determined by the length of the active element, which is nominally ½ the wavelength of the signal. A signal propagating through a wear plate that is ¼ of a wavelength thick will produce a backwall echo that is in phase with the initial excitation pulse (GE Panametrics, 2003). The amplitudes of the in-phase signals will be additive, thus increasing the amplitude of the signal that enters the specimen.

Ultrasonic transducers usually transmit either longitudinal or shear waves (GE Panametrics, 2003). Longitudinal wave transducers are more commonly used for standard thickness gauging and flaw detection because longitudinal waves propagate through liquid couplants while shear waves do not. However, in cases where calculations of Young's Modulus or Poisson's Ratio are desired, shear wave transducers are often practical.

Transducer selection is often dictated by the acoustical characteristics of the test specimen. The signal frequency is the primary factor in determining the most practical transducer for a given specimen. Low frequency ultrasound signals have better penetration than high frequency signals in a highly attenuating or highly scattering material (Fowler et al., 2003). Thus a low frequency transducer would be the best choice for measuring a thick specimen with inherent small discontinuities. However, low frequency signals have a longer waveform that inhibits resolution. High frequency signals produce short waveform echoes, which enable better accuracy in measuring delay time (Fowler et al., 2003). Thus, when either a high resolution of flaw location or an extremely accurate thickness measurement is desired, high frequency transducers are most practical.

Measurement Methods

While a transducer is crucial to generating ultrasonic signals, it must be incorporated in an electronic measurement system in order to enable signal processing. The basic ultrasonic measurement system consists of a microprocessor, a pulser, a transducer, an amplifier, and an oscilloscope. The microprocessor-controlled pulser provides a broadband voltage impulse to the ultrasonic transducer. The transducer converts the electrical impulse to an ultrasonic pulse signal that is introduced to the test material. Reflected signals from the specimen are received by the transducer, converted back to electrical pulses, and then fed to an amplifier. Time domain observations of the signals can then be made using an oscilloscope.

Measurement of the ultrasonic signal transit time through the test piece is the basis for ultrasonic thickness gauging and flaw detection. Thickness and location calculations can be accomplished using the relationship expressed in equation 4.4. It is apparent that accurate calculations can be made only by obtaining accurate measurements of the transit time. Several methods for measuring the signal transit time exist using the previously described ultrasonic system.

The most basic method is to measure the time between the excitation pulse and the first backwall echo. Because the excitation pulse occurs at time $t = 0$, the time of the echo pulse reception would essentially be the round-trip transit time of the signal through the specimen. However, in reality, an offset needs to be subtracted from the measured time to account for the transit time of the pulse through the transducer wear plate and the couplant, as well as the rise time of the signal and any electronic switching time or cable delays (Fowler et al., 2003). Thus, this method may not be the most accurate as it requires gage calibration which may be subject to some error.

Another possibility is to measure the time difference between the reflection from the front surface of the test piece and the first backwall echo. This method would eliminate the need to subtract a calibrated offset. However, for direct contact transducers, the waveform of the front surface reflection is often hard to distinguish because the reflection occurs very soon after the excitation pulse. At this time, the transducer element may still be vibrating and some internal reflections may occur. The signal generated by the front surface reflection will be corrupted by the internal noise, making an accurate time measurement difficult. Additionally, if the impedance of the wear plate and the couplant is similar to that of the test piece, the amplitude of the reflection will be quite small. One technique for improving the accuracy of this method is to use a delay line transducer, which couples the active element to the test piece with an extended plastic block. The plastic delay line allows the element to stop vibrating before the first reflected signal is received (GE Panametrics, 2003). Thus, the time of this reflection can be measured because the signal is easily distinguished.

The most accurate method for determining the signal transit time is to measure the time difference between the first backwall echo and successive backwall echoes. This method requires no offset and the first backwall echo usually occurs after the active element has stopped vibrating. In order to utilize this method, the specimen must have low acoustic attenuation and high impedance (creating high energy reflections) so that multiple backwall echoes may occur.

4.2 Laboratory and Field Tests

Transducer Calibration

Before incorporating any ultrasonic testing devices into the beam crawler design, several basic laboratory and field tests were performed to evaluate both the thickness gauging and the flaw detection capabilities of the available ultrasonic equipment.
An initial calibration test was used to determine the transducer offset created by electronic delays and signal transit time through the couplant and wear plate. The ultrasonic measurement system consisted of a GE Panametrics direct contact videoscan transducer, a GE Panametrics pulser/receiver, and an HP digitizing oscilloscope. The oscilloscope was interfaced to a PC and controlled by a LabView program through the use of a GPIB. The videoscan transducer produced a 1MHz heavily damped broadband signal, which provided good resolution due to the short signal waveform.

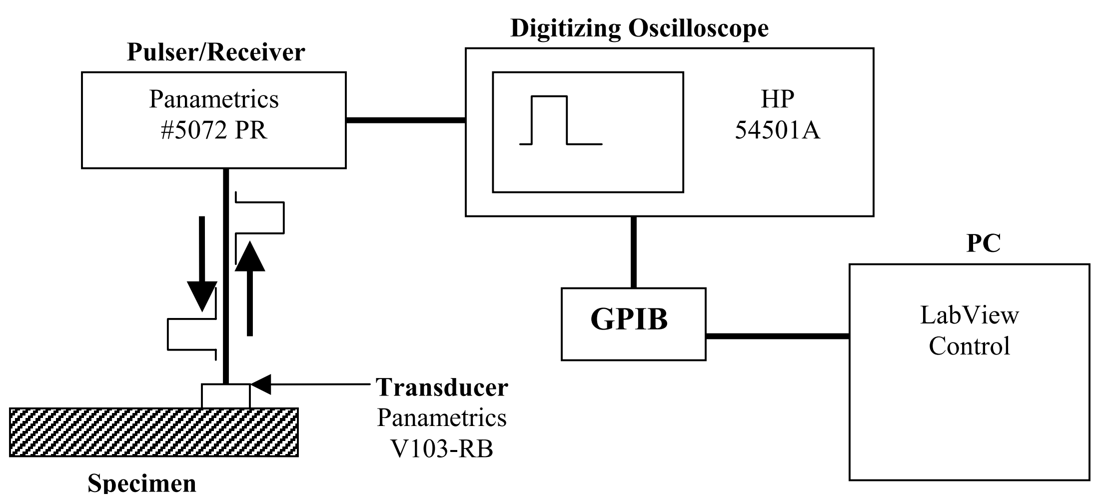

Figure 4-2. Ultrasonic measurement system block diagram.

Calibration was achieved by applying the transducer to several steel slabs of varying thicknesses. The transducer was coupled to each steel surface using Vaseline®. Figure 4-3 shows the ultrasonic signal produced when the transducer is applied to a 25mm-thick steel slab. The high impedance of the slab (relative to the impedance of air) creates multiple backwall echoes. Based on the data sample rate of the LabView program, the time between successive echoes can be measured accurately to 0.1 microseconds. The following equation represents the method for obtaining the gage offset:

Equation 4.5 $$t_1 - \Delta t = \delta$$

t_1 = Time of first backwall echo
Δt = Time between first and second backwall echo
δ = Gage offset

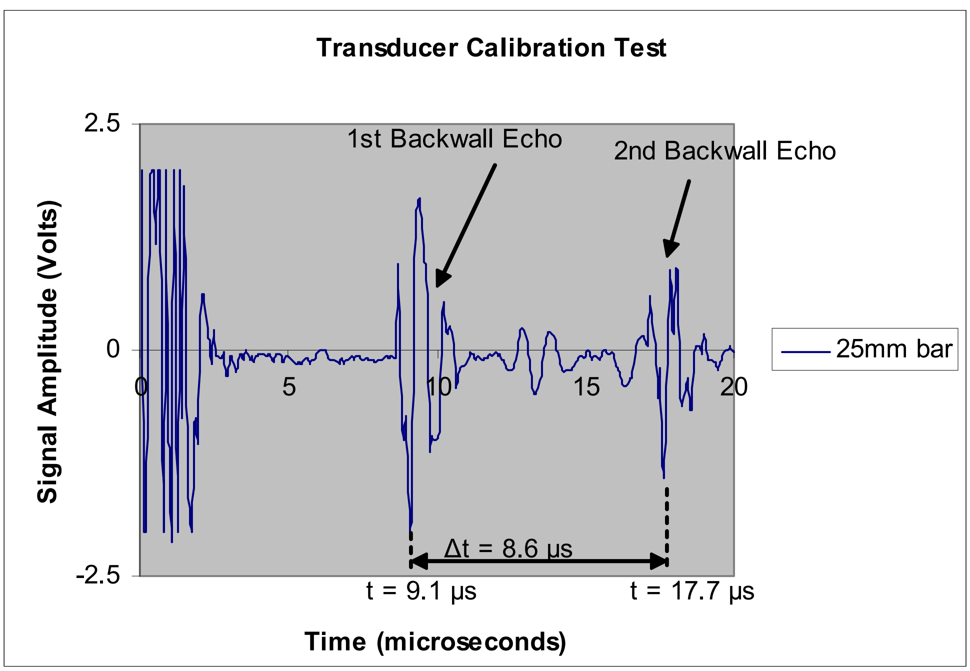

Figure 4-3. Transducer calibration signal.

For the 25mm steel slab, the time between successive backwall echoes is 8.6 microseconds. The first echo occurs at 9.1 microseconds. Thus the gage offset is 0.5 microseconds. This calibration procedure was repeated on multiple steel test slabs and the gage offset was constant for all thicknesses.

Once calibration was accomplished, thickness measurements of several steel slabs were performed to assess the accuracy of the ultrasonic measurement system and the reliability of the gage offset. Both caliper measurements and ultrasonic measurements were made for each specimen as a means of comparison.

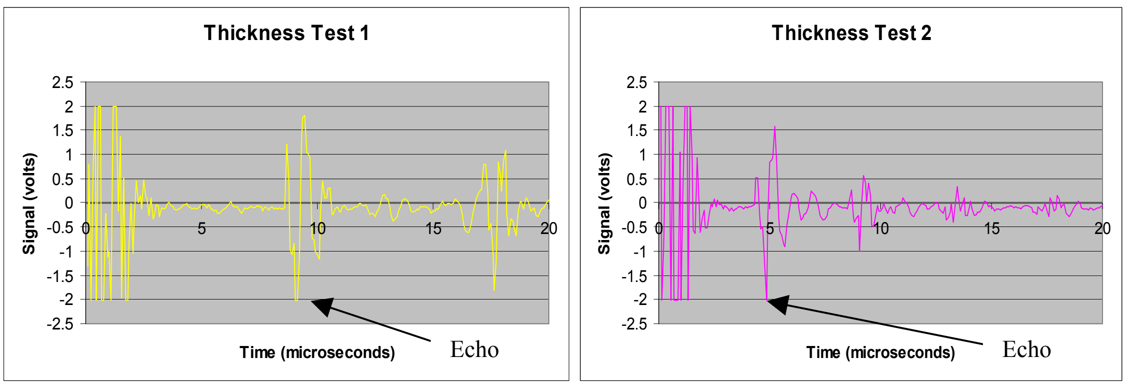

Caliper measurement: 25.4 mm
Ultrasound measurement: 25.5 mm

Caliper measurement: 12.8 mm
Ultrasound measurement: 12.7 mm

Figure 4-4. Comparison of caliper measurement and ultrasonic measurement of two steel slabs.

Ultrasonic measurement calculations were performed using the sound velocity for steel, 5.92 mm/μs, and Δt. The time between the excitation pulse and the echo pulse, Δt, was established by subtracting the offset from the measured echo pulse time for each specimen. Figure 4-4 shows the ultrasonic signals generated by two measurements and the corresponding comparisons between the calculated ultrasonic values and the caliper measurement values. It should be noted that the resolution of the ultrasonic measurements was determined primarily by the sample rate of the LabView program.

Caliper measurements and ultrasonic measurements agreed within 0.1mm for specimens over 10mm in thickness. As the ultrasonic method provided satisfactory thickness measurements in the laboratory, the ultrasonic measurement system was transported to the LaPlatte River Bridge to demonstrate the thickness gauging capabilities of the system in field tests. The transducer was applied to several locations along a steel girder. Calculations of the varying flange thicknesses were made using the data collected at the site and the established gage offset. Figure 4-5 shows the ultrasonic measurements of two flange thicknesses.

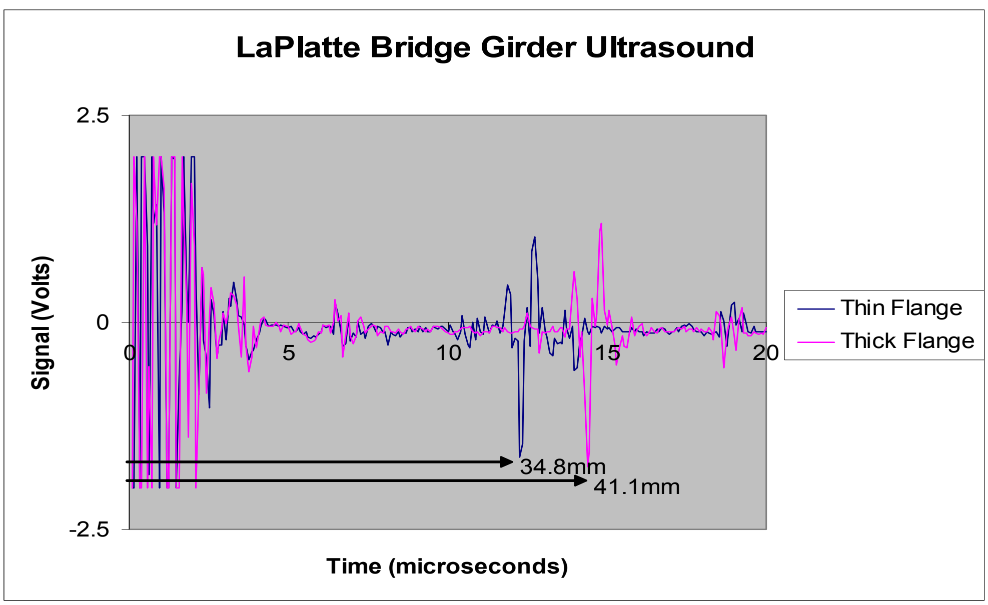

Figure 4-5. Field test thickness gauging.

Transducer Sensitivity and Resolution

In addition to thickness gauging tests, several flaw detection tests were performed in the laboratory. The transducer sensitivity to embedded defects was evaluated by applying the transducer to a specimen with a simulated internal crack. Two steel plates of different thicknesses were clamped tightly together. The thin gap between the two plates simulated a small crack parallel to the surface of the specimen. The transducer was applied to both sides of the specimen to provide different flaw depth measurements. Figure 4-6 shows the ultrasonic measurements taken from both sides of the specimen. It is apparent that most of the signal energy is reflected at the gap, while very little energy is transmitted through the boundary. In both cases, multiple echoes occur at the gap while no backwall echo occurs. If a backwall echo did exist, it would occur at about 12.5μs (this corresponds to the 36mm overall thickness of the specimen) in both cases. However, neither measurement shows any indication of such a reflection.

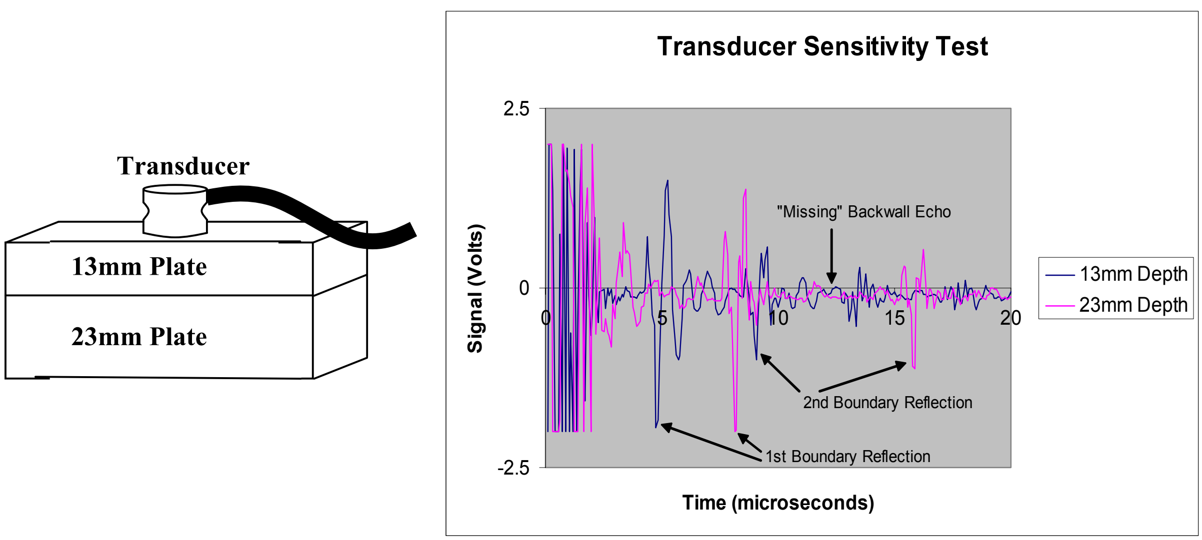

Figure 4-6. Sensitivity test.

The axial resolution of the transducer was tested by using a specimen with a thin crack lying perpendicular to the surface. A 1mm-wide by 13mm-deep crack was cut into the surface of a 25mm-thick steel plate. The transducer was coupled to the opposite surface such that the crack was aligned with the center of the transducer. Figure 4-7 shows a comparison between the ultrasonic measurements of a plate without the crack and the plate with the crack. A reflection occurs at the base of the crack. The energy loss of the reflected signal compared with the backwall echo is about -5.8 dB, or about 50 percent of the amplitude of the echo signal. Thus, the reflection caused by the 1mm wide crack is relatively large.

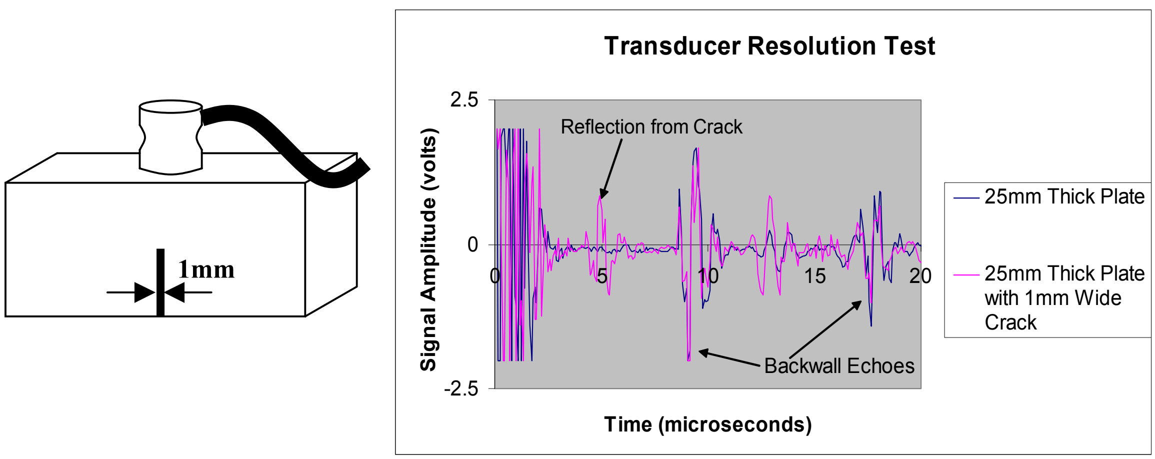

Figure 4-7. Resolution test.

4.3 The Articulated Ultrasound Robot Arm

Design

While incorporating ultrasonic measurement into an autonomous inspection system has many advantages over traditional ultrasonic measurement methods, the primary advantage is enhanced accessibility. As an example, in the previous on-site ultrasonic tests at the LaPlatte River Bridge, the simple task of coupling the transducer to a beam flange required the use of a 20-foot ladder to access the location. An autonomous system with the ability to couple the transducer to the flange could perform the same task with much greater ease.

The primary requirement for integrating an ultrasonic system with the beam crawler was to design an articulated ultrasonic robot arm (AURA) that could couple the transducer to the surface of a specimen. Additionally, the AURA needed on-board power and control. Results from the transducer sensitivity and resolution tests indicated that the signal produced by the available transducer would rapidly attenuate in small air gaps. Thus, sufficient force would also be needed to ensure coupling without any signal loss.

A high-torque servo was chosen as a means of providing the necessary coupling force for the AURA. The servo arm was incorporated in a four-bar system that could raise and lower the transducer relative to an overhead surface. The transducer was mounted in a drilled-out aluminum block that was fastened to a vertical bar. The transducer block was pinned so that some rotation in a vertical plane could occur. Additionally, a thin layer of foam was placed between the transducer and the aluminum block to enable further movement. The mobility provided by the foam and the rotating block allowed sufficient coupling by countering any initial misalignment between the transducer wear plate and the test surface. The four-bar system, fastened to a wooden mount, could be placed in the beam-crawler chassis to provide measurement of the

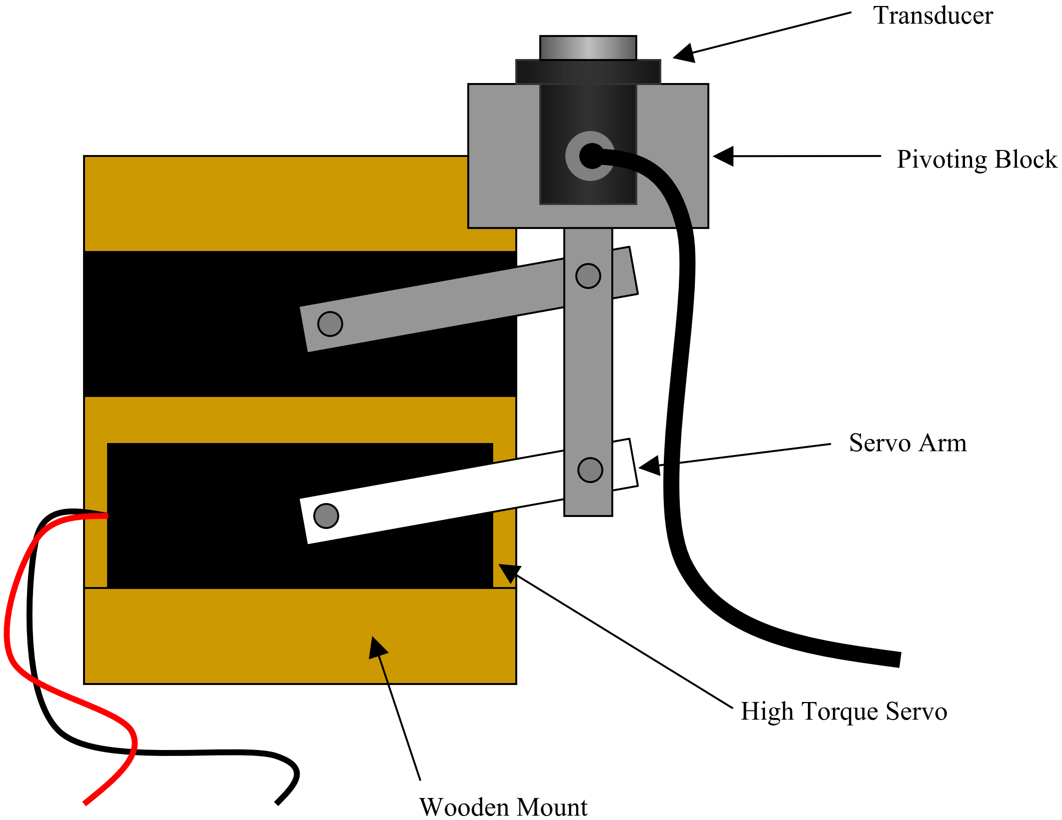

Figure 4-8. The Articulated Ultrasound Robot Arm.

overhead beam flange. The servo was connected to the steering channel of the drive train receiver. This channel was available as steering was not necessary for operation of the beam-crawler. While the servo could be powered by the receiver, the large current draw during high torque applications necessitated the use of a separate battery pack to avoid any overload problems. A low-power AURA based on a 6-bar toggle mechanism was designed, but not implemented due to the feasibility of the simpler 4-bar design.

Tests

In preliminary tests where the beam crawler was mounted on a steel beam, the AURA was controlled with the steering signal from the radio-control transmitter. However, problems occurred when the transducer was coupled to the steel beam. The transmitter signal, which propagated through the beam, interfered with the transducer signal when coupling occurred. The interference was so great that no ultrasonic signal could be distinguished on the oscilloscope display. The only solution to this problem was to find another method for controlling the AURA that did not employ radio frequency signals.

Another option for control was to utilize the Jackrabbit microcontroller. The Jackrabbit was already programmed to send pulse width modulation (PWM) signals from a digital output port. A modification in the program changed the pulse width of these signals to match those necessary for control of the AURA servo. Additionally, once the AURA servo was connected to the Jackrabbit output port, the program was further modified so that coupling would be triggered by the peripheral photo sensors.

Control by the Jackrabbit proved to be successful. The beam crawler was again mounted on a steel beam. This time, however, the photo-sensors were used to actuate the AURA. Several trials were performed and ultrasonic thickness measurements were achieved. Figure 4-9 shows ultrasonic data collected during AURA tests.

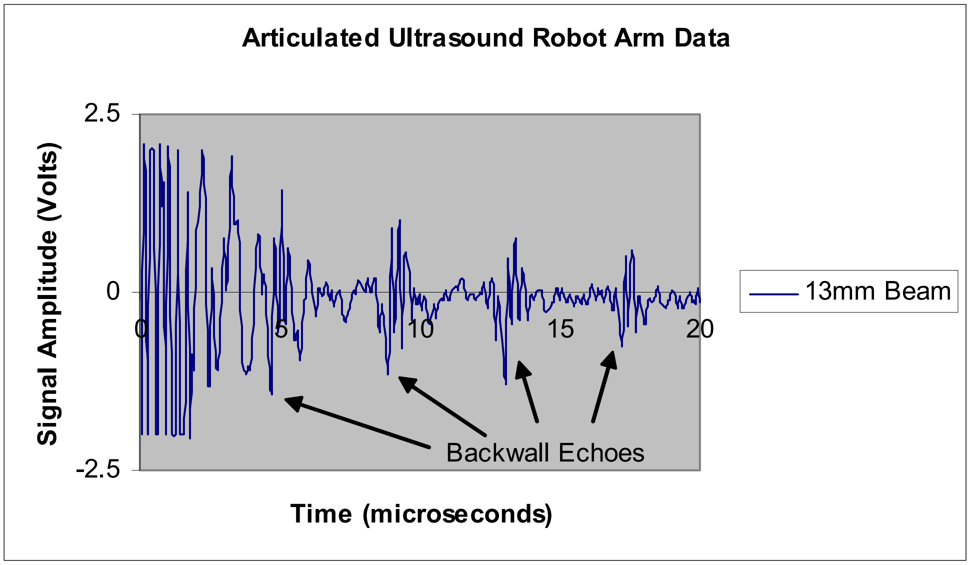

Figure 4-9. AURA sampling of a 13mm thick steel beam.

Results

The ultrasonic system employed in the AURA tests proved to be sufficient for acquiring data relevant to structural health monitoring. However, this system was used because it was available. Practical implementation of robotic ultrasonic inspection would necessitate the use of a modified ultrasonic system.

The type of couplant used is important to the effectiveness of an ultrasonic system. Most transducers rely on couplants for signal penetration. During the AURA tests, the Vaseline® would remain on the transducer to provide sufficient coupling for multiple trials. However, it is likely that any viscous couplant would eventually wear away during long-term deployment. A plastic delay line or a sealed gel pad might be more practical for long-term field deployment. These couplants do not deteriorate rapidly after prolonged contact.

Transducer selection is also important for effective ultrasonic measurement. The optimal choice depends on the application. The signal frequency, waveform, and wave type can be varied to maximize penetration, resolution, or sensitivity. The AURA transducer, with its mid-level frequency and short waveform, had both moderate penetration and resolution. However, for measuring thick samples, a lower frequency transducer might be more practical. Conversely, better sensitivity to small defects would require a higher frequency transducer.

Most importantly, the size and transportability of the ultrasonic system determine its effectiveness as a mobile inspection unit. While the ultrasonic system of the AURA provided accurate and repeatable measurements, it was impractical for field tests. The on-site tests that were performed required time and effort in transporting and assembling the bulky system, which included an oscilloscope, a PC, and a portable power supply. Furthermore, the inability to incorporate such a system for on-board use meant that the effective operating range of the robot was limited by the length of the transducer cable. A smaller system would be more practical for long-term field implementation. Several portable ultrasonic inspection systems do exist that include both thickness gauging and flaw detection capabilities. It would be feasible to mount a portable unit on a mobile robotic platform.

Figure 4-10. Portable ultrasonic thickness gage (CHECK-LINE^{TM} TI-25M-MMX).

While the ultrasonic system employed for the AURA testing may not have been ideal for practical inspections, it was sufficient for demonstrating the feasibility of the AURA design. The AURA tests indicated that the beam-crawler could possess effective advanced inspection capabilities, including the use of nondestructive evaluation instrumentation. Furthermore, the actuation by peripheral sensors showed that the ultrasonic device could have autonomous capabilities as well.

Chapter 5
Future Applications of Robotic Systems

The process of developing a task-specific mobile robotic platform provided much insight into the general design of robotic inspection systems. This chapter will discuss the results from performance tests of the autonomous beam-crawler and their implications for future applications to structural health monitoring as well as other tasks.

5.1 The Autonomous Beam-Crawler

Performance

The beam-crawler project had two primary objectives: to design a mobile robotic platform that could be outfitted with various inspection devices specific to structural health monitoring, and to create an autonomous system capable of responding to environmental stimuli. Both of these objectives were accomplished.

Field tests demonstrated that the beam-crawler could operate autonomously in an environment outside of a laboratory. Adaptability is the key to any successful autonomous system. A robot can be programmed to perform a certain task. However, if the environment in which it is operating changes slightly, the robot will fail to perform unless it can either be reprogrammed or respond and adapt to those changes. In situations where long-term deployment or long-range operation is desired, reprogramming a robot becomes highly inefficient. Adaptability is extremely important for long-term performance in an uncontrolled environment.

While the beam-crawler may have been capable of only a primitive form of adaptability, it did demonstrate an ability to respond to environmental stimuli. The peripheral photo-sensors could detect objects placed on the beam flange and elicit a response from the robot when such objects were encountered. The placement of objects on the flange could determine both the location and the number of inspections performed by the robot.

The beam-crawler may not have been able to adapt to complex environmental changes. For example, it could not negotiate a bridge abutment in order to operate on multiple sections of the span. However, it did possess the adaptive characteristics necessary for operating within an array of embedded or mounted sensors. By responding to the location of individual sensors (as determined by the placement of trigger objects), the beam-crawler could adapt to the size of the array as well as changes in the location of sensors in the array.

Once the beam-crawler was established as an autonomous system, its capabilities as a mobile platform were tested. First, incorporating a wireless video camera demonstrated the ability for visual inspection enhancement. While the camera enabled visual access to remote locations, a device that could provide more advanced information about sub-surface characteristics was desired. Successfully incorporating such a device into the autonomous system would prove the beam-crawler as a practical mobile platform.

The design and fabrication of the Articulated Ultrasound Robot Arm (AURA) created a potential means for providing sub-surface inspection capabilities to the beam-crawler. Initial tests of the AURA signified some difficulty integrating the device with the radio-control system. However, reprogramming the processing system of the beam-crawler not only allowed the AURA to be incorporated successfully, but it also enabled the device to acquire a degree of autonomy. By connecting the AURA directly to the control system, the peripheral photo-sensors could actuate the servo arm and couple the ultrasonic transducer to the beam. Thus, the ultrasonic inspection system could be controlled by placing objects in the light path of the photo sensors.

While the ultrasonic measurement system used for the AURA tests may not have been practical for field-deployment, it did provide a means for testing the advanced platform capabilities of the beam-crawler. The beam-crawler proved to be not only moderately adaptive, but also capable of providing a platform for sophisticated sub-surface inspection devices.

Enhanced Inspection Capabilities

The beam-crawler provides a few general improvements in inspection capabilities over some of the remote-control systems currently employed in structural health monitoring. Remote-control systems are often limited in operation by the length of tethering power and control cables or the range of radio frequency transmitting devices. Because the beam-crawler operates autonomously, carrying a power supply, it is only limited by battery capacity. Based on the operational range estimates in section 3.4, the beam-crawler currently has the capacity to operate for almost a kilometer before performance is affected by inadequate power. This range would be sufficient for operation on most bridges and structures. Additionally the capacity of the power supply could be more than quadrupled with only minor modifications to the drive system.

The adaptive nature of the autonomous system creates the potential for long-term deployment. Remote-control systems require the continuous guidance of an operator. Thus, long-term deployment of remote-control systems is impractical because it requires prolonged human supervision. In contrast, the long-term deployment of an efficient autonomous system requires time and effort only in the initial stages of setting up the system. Once the system is in operation it can provide continual surveillance with little additional human guidance.

The concept of a mobile platform also enables certain adaptability within the system. Rather than developing a system capable of only one method of inspection, a robot that can be outfitted with a variety of instruments provides numerous inspection capabilities. Many currently employed inspection systems are designed to provide one or two specific methods. A robotic platform can be adapted to provide the optimal method for a given structure.

While the beam-crawler may be a simplistic model of an autonomous robot, as a proof-of-concept, it elucidates many of the benefits provided by the application of autonomous systems to structural health monitoring.

The Next Generation of Beam-Crawler

The beam-crawler has limitations in utility because it is designed for one span of a specific structure. However, the next generation of beam-crawler could address this issue by providing a design that allows generic implementation. Small variations in bridge geometry do not present a significant challenge for widespread use. For example, flange width and thickness, and diaphragm clearance can all be accounted for with only minor modifications to the current design.

The primary challenge is to overcome the limitation in mobility. Currently, the beam-crawler is limited to operating on one span of the bridge because it is not designed to move around a pier or abutment. Additionally, some bridges may present a geometry that does not permit the use of a suspended crawler as a result of diaphragm-to-girder attachments that leave no clearance on the top surface of the flange. One potential solution for these scenarios is to use magnetic coupling.

As shown in section 1.2, there are several developing technologies that employ magnetically coupled robot inspectors. Magnetic wheels, tracks, and feet for various crawlers and walkers enable mobility with access to only one surface. Furthermore the use of articulated limbs creates the potential for negotiating right-angle joints.

It should be taken into consideration, however, that the use of magnetic coupling and articulated limbs poses many further challenges. The current beam-crawler design that utilizes a suspended chassis does not require steering for operation because the geometry of the bridge constrains the range of motion. Implementing magnetically coupled robots that have contact with only one surface would require a more complex processing system to account for the steering and directional control that would be necessary. Additionally, magnetic drive systems could create severe restrictions in payload size and robot weight. Allowing for an increase in these two factors would mean using stronger magnets that supply a greater normal force. Yet, it is also necessary to account for the power used for decoupling. Stronger magnets require greater force for decoupling. This leads to increased power consumption in the system. These are all factors that should be considered when progressing to a more complex design.

A different approach to overcoming the challenges created by generic use would be to implement the current design on a large scale. If the suspended design is applicable to most bridges, the mobility limitation of operating on one span could be overcome by deploying multiple units. The relatively simple design of the current generation beam-crawler creates a low-cost system. Using several beam-crawlers at one location could provide coverage of the entire structure while still enabling long-term deployment capabilities. The concept of large-scale implementation could be feasible with this type of low-cost system. The limitations in mobility and control of a single unit would be insignificant with the deployment of multiple beam-crawlers.

The concept of utilizing multiple low-cost units at one site could perhaps provide the solution that is most feasible for short-term development. In addition to the simple design and low cost of these units, a further benefit of large-scale use is the ease of replacement in the event of a failure. Highly complex systems can be costly to repair. Additionally the deployment of only one unit creates severe limitations if the inspection system is inoperable during repairs. Large-scale system inspection capabilities may be affected by the loss of one unit, but these systems can still be effective. The question of whether the cost benefits of large-scale deployment outweigh the sophisticated control capabilities and high mobility of more complex designs may be answered with long-term development of advanced autonomous systems.

5.2 High-Mobility Systems

The Unmanned Aerial Vehicle (UAV)

The insight provided by the development of the beam-crawler suggests that inspection systems that increase the efficiency of an inspection operation either by improving the accuracy of assessments or by minimizing the use of human resources may prove to be most valuable. While application of advanced inspection methods such as sub-surface nondestructive evaluation may enable the most accurate assessments of structural health, a highly mobile robotic platform could provide a greater efficiency in visual inspections.

The beam-crawler demonstrated some of the benefits of enhanced visual inspection by providing close-up images of low-accessibility locations. A robotic platform with even greater mobility than the beam crawler could further enhance visual capabilities by accessing more remote locations.

Greatest mobility can be achieved with an aerial platform. Efforts to develop aerial robotic platforms, such as the Caltrans project discussed in section 1.2, are currently underway. However, no such systems have been routinely employed.

Because the movement of the beam-crawler was constrained by the geometry of the structure, autonomous operation was relatively simple to enact. However, an aerial platform, which has few mobility constraints, is much more difficult to design as an autonomous system. Nevertheless, some of the design concepts of the beam-crawler could be applied to an aerial platform.

(a) (b)

Figure 5-1. (a) Hovering Helibot. (b) Mounted Camera.

The Unmanned Aerial Vehicle (UAV) Helibot was based on the concept of utilizing an off-the-shelf radio-controlled system as a platform for visual surveillance instruments. A mid-level performance radio-controlled helicopter (Ikarus^{TM} Piccolo Fun Micro Helicopter) was purchased to provide an aerial platform for mounting a small wireless camera. Because the performance of the helicopter was greatly affected by weight, the camera needed to be lightweight to allow flight. A 9-gram wireless camera transmitting at a frequency of 2.4GHz was mounted to the underside of the helicopter body. Power was supplied to the camera from the R/C receiver of the helicopter. The camera receiver was linked directly to a laptop to provide real-time images.

Several trial runs were performed with the UAV Helibot. The Helibot proved to operate effectively inside enclosed structures (i.e., in buildings) as well as outdoors. However, it should be noted that outdoor operation was only feasible in relatively calm conditions. Strong wind gusts would adversely affect control of the system. The mounted camera was light enough so that it did not substantially hinder performance. Images could be obtained by allowing the helicopter to hover in proximity to a structure.

Figure 5-2. Typical image obtained from Helibot camera.

The primary limiting factor in the effectiveness of the Helibot was the operator skill. As a novice operator, the UAV Helibot proved to be extremely difficult to control, requiring much practice before any practical inspections could be performed. Due to the low weight, high torque, and unrestricted motion of the system, the UAV was quite sensitive to small adjustments of the transmitter controls. Furthermore, the low weight of the vehicle and the lack of protection for the rotors sacrificed the durability of the system. Minor collisions could result in considerable damage to the Helibot (fortunately, not to the structure).

One of the improved features of the UAV helibot over a tethered aerial platform is enhanced mobility and range of operation. Aerial platforms tethered by a power cable are limited by the length of the cable. Furthermore, movement can be somewhat restricted as cables become entangled by the structure. The Helibot allows a full six degrees of freedom (i.e., latitude, longitude, altitude, pitch, roll, yaw) and an operating range limited only by the transmission range of the radio signal.

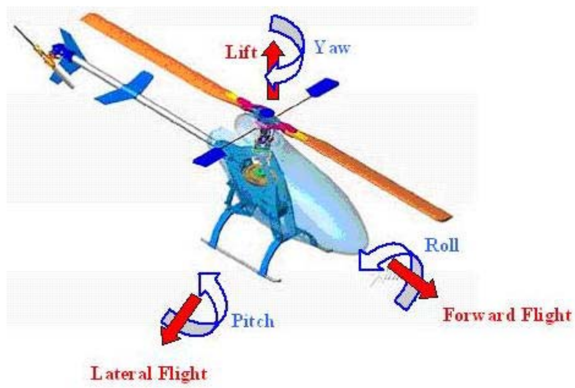

Figure 5-3. Diagram of UAV degree of freedom.

While the UAV Helibot may prove to be an effective inspection system if operated by skilled personnel, a system that is more durable (i.e., resistant to impact) and requires less training for operation may be more practical for widespread use.

UAV Airship

One possible candidate for a more robust and more easily operable system is the radio-controlled airship, or blimp. Airships may be more suitable than helicopters as mobile platforms for several reasons.

Airships are naturally buoyant. Typically, small (~ 6 to 8 feet) RC blimps have non-rigid envelopes that are filled with helium to provide buoyancy. Neutral buoyancy can be achieved through small adjustments to the weight of the ship. A neutrally buoyant blimp would provide a highly stable platform for cameras or other instruments because little control is necessary to maintain a fixed position. In contrast, a helicopter requires continuous adjustment to provide a stable hovering platform.

Another advantage of the airship is maneuverability at low speeds. The power system consists of usually two or three micro-electric motors that can rotate to supply vectored thrust from the attached rotors. Because vectored thrust can be applied at low speeds, the sensitivity to small motor control adjustments is decreased. This decreased sensitivity could provide greater maneuverability in confined spaces.

Airships also have low power consumption because little power, if any, is needed to maintain buoyancy. This low consumption enables a relatively long operation time with a small, lightweight battery pack. Additionally, low power consumption makes blimps good candidates for renewable power sources such as solar power.

(a) (b)

Figure 5-4. (a) Typical R/C Blimp (Tri-Turbofan Airship). (b) Propulsion system (note protected rotors).

It is also possible that blimps would be more resistant than helicopters to damage from impact. The small helical rotors of blimps are not as likely as the large helicopter rotors to come into contact with the structure under surveillance. In the event of a collision, the envelope, which is usually constructed from Mylar™, would probably bear the impact. Thus, the minimal exposure of the mobility components to impact would decrease the likelihood of damage affecting the overall performance of the ship.

While the inspection capabilities of blimps are yet to be fully tested, there are likely to be drawbacks to using blimps as well. For example, even the smallest blimps are several feet long. This requirement is necessary to provide a large enough volume of helium to counterbalance the weight of the electronic components and power system of the ship. This large volume may not allow operation in areas that are extremely confined. Furthermore, like the helicopter, the low weight of the blimp makes it extremely sensitive to wind. Thus the location and design of a structure and the conditions of the environment may limit the effectiveness of an airship.

Autonomous UAVs

While the range of motion of unmanned air vehicles presents significant challenges for employing autonomous control, there are steps being taken towards developing autonomous UAVs. Airships, in particular, are also good candidates for autonomous control. Their stability would simplify control programming and their low power consumption could enable long-term deployment.

In recent years, the University of Virginia developed a semi-autonomous solar powered airship (Turner). The 20 meter airship was designed to receive user inputs transmitted from a ground station. The on-board hardware system consisted of an embedded computer linked to a GPS receiver and attitude sensor. Thus, user inputs of location (latitude, longitude, altitude) and attitude (pitch, yaw, roll) could actuate a system of servo motors that would provide the appropriate vectored thrust to achieve the desired location and attitude.

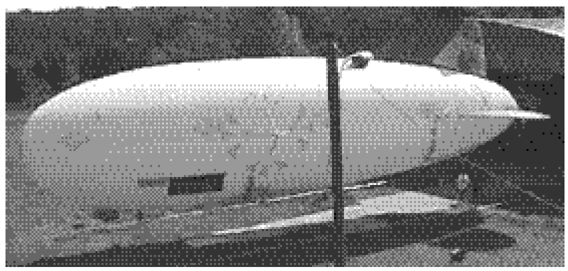

Figure 5-5. University of Virginia solar airship *Aztec*.

Researchers at the Robotics Institute at Carnegie Mellon have also developed a semi-autonomous airship for collection of environmental data (Kantor et al., 2001). Researchers have employed a nine-meter airship as a mobile platform for environmental sensing. The objective of the project is to develop a solar-powered airship capable of long-term deployment. This airship would carry a payload of sensors to monitor environmental parameters such as air quality, water quality, and extent of defoliation. The airship is a suitable platform for this project because it provides stability for sensing operations that require a relatively long sample time. Also, blimps provide an excellent means for monitoring areas, such as wetlands, which are difficult to access from the ground.

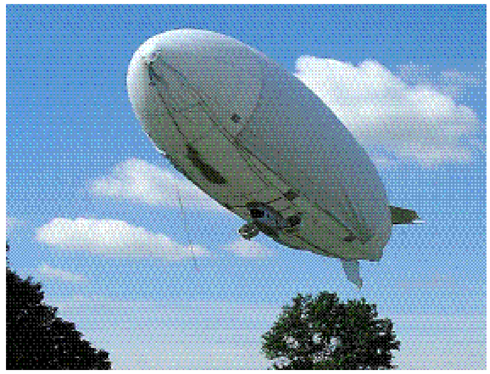

Figure 5-6. Airship platform for environmental sensing (Kantor et al., 2001).

5.3 Beyond Structural Health Monitoring

The basic principles of robotic systems have a variety of applications outside of structural health monitoring. Concepts such as long-term deployment and continual surveillance can be applied to tasks where the use of human assets is impractical due to costs or ineffective due to human limitations such as fatigue. Robotic systems can also find applications in situations where surveillance or assessment of inaccessible locations is necessary. Finally, the expendable nature of robots makes them highly appropriate for tasks that require human deployment in hazardous locations. The following are examples of current applications of these concepts.

Surveillance and Long-Term Deployment: Robotic All-Terrain Vehicles

The Cyberscout project at Carnegie Mellon University involves the development of a mobile robotic platform for reconnaissance, surveillance, and security operations in primarily military applications (Dolan et al., 1999). Because these operations can be time-consuming, monotonous, and often dangerous, robotic scouts may prove to be a practical and effective replacement for humans.

Researchers have retrofitted commercial All-Terrain Vehicles (ATVs) to serve as mobile platforms. The automation of throttle, steering, braking, and gearing functions creates the potential for autonomous operation of the ATVs. Computational control of the ATVs is provided by a set of networked computers, which can perform low-level processing for locomotion and high-level processing for planning, perception, and communications. Navigation is accomplished using a GPS, while multiple cameras provide vision for obstacle avoidance, landmark tracking, and surveillance.

Figure 5-7. Robotic ATV (Dolan et al., 1999).

While still in development, the robotic ATV has great potential for military and security applications. The range capabilities (~ 200 miles per tank of gasoline) could allow for long-term deployment and surveillance. Ultimately, robotic ATVs could be deployed in groups for tactical purposes (Dolan et al., 2003). In the event of a "stakeout", communication between autonomous vehicles could be used to provide optimal vehicle positioning around a site of interest.

Low Accessibility: The Reconfigurable MiniRover

Outside of structural health monitoring, another practical application of robotic systems for assessment of inaccessible locations is in space exploration. Researchers at NASA's Jet Propulsion Laboratory are developing miniature exploratory robotic vehicles (minirovers) for deployment on planetary surfaces (Trebi-Ollennu and Kennedy, 2002). The Reconfigurable MiniRover would provide a mobile platform for a variety of sensors used in surface exploration. Due to its low weight and small size (10 to 20kg with a 20cmx40cm footprint), the minirover could be man-portable. The robust design, which includes a drive shell that also serves to protect the electronics and sensor payload, could enable ballistic deployment.

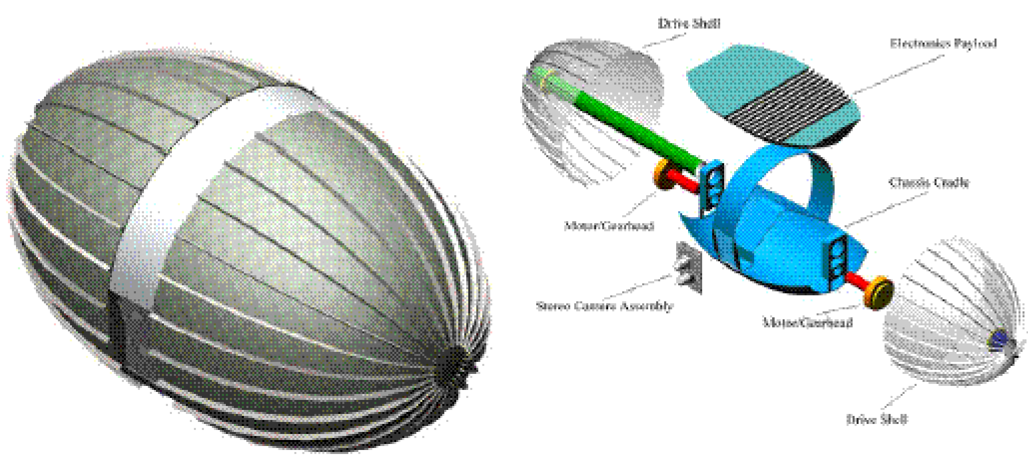

(a) (b)

Figure 5-8. (a) Assembled minirover. (b) Various minirover components (Trebi-Ollennu and Kennedy, 2002).

A further application of the minirover design is in smart sensor webs (Trebi-Ollennu and Kennedy, 2002). Deployment of a team of minirovers, each possessing one primary sensing mode and a means for communication, could provide the same surface exploration capabilities as a single, larger and more complex mobile robot. The advantage of using a web of simple robots versus a single, multi-purpose robot is the decoupling of sensor modes. The failure of a single unit in the minirover web would be unlikely to cause system-wide failures. This is not always the case with single, multi-function robots where failure of one component often affects overall system performance. Furthermore, surface coverage of a system of mobile robots is far greater than that of a solitary unit.

The concept of mobile robots as smart sensor webs is similar to that of embedded sensor networks where a system of single-function sensors provides a holistic approach to obtaining information. However, the greatest difference in utilizing mobile robots instead of embedded sensors is the adaptability provided by mobile units. While embedded sensors are fixed in location, mobile robots create a web that can be adapted to optimize valuable information about a structure or site.

Hazardous Locations: Urban Search and Rescue

Search and rescue poses many potential hazards to human or canine assets (Murphy et al., 2000). Catastrophic events occurring in urban locations often result in the collapse of large man-made structures in highly populated areas. Conventional search and rescue methods in these situations entail the deployment of rescue workers into collapsed structures, which may be unstable and prone to further deterioration. Thus, improvements in urban search and rescue (USAR) methods would not only benefit the health of survivors, but also the safety of rescue personnel.

Currently, the University of South Florida is host to a center for robot-assisted search and rescue (CRASAR), which aims to improve USAR methods by utilizing robotic assets (Murphy et al., 2000). Mobile robots could provide assistance in site reconnaissance as well as victim identification and localization. The value of USAR robots depends on the extent of the robot capabilities.

For a non-autonomous remote-control robot, reconnoitering a disaster sight requires mechanical adeptness as the terrain is usually uneven and it often presents many obstacles. However, most remote-control methods are not practical at USAR sites (Murphy et al., 2000). Tethering cables can quickly become tangled in debris or other objects. Radio frequency communication is often not possible due to the large amount of shielding material in a collapsed structure. Additionally, in the event of a bombing, radio communication is suspended in order to prevent the potential triggering of other explosives. Due to the restrictions on tele-operation, robots with some degree of autonomy are desirable.

In addition to the intelligence and mobility required to negotiate rugged terrain, USAR robots could have further sensing capabilities (Murphy et al., 2000). Victim identification might be achieved through the use of thermal or carbon dioxide sensors. Air quality monitoring would be useful in a reconnaissance mission to determine whether a location is safe for rescue workers. USAR robots might also carry tools for stabilizing structural integrity or for penetrating inaccessible locations. Thus, the concept of a mobile robotic platform for sensors and equipment could be applied to search and rescue methods.

5.4 Future Robotic Designs

While robotic aerial platforms may provide enhanced mobility, the use of ground vehicles (i.e., rovers, crawlers, climbers, etc.) may prove to be more effective in many situations. For example, aerial platforms may be impractical for use in extremely confined spaces, such as those found at USAR sites. Military and security operations may require stealth vehicles to complete surveillance tasks. Ground vehicles may provide a better means than aerial vehicles for enabling undetected operation. While ground vehicles have many mobility limitations, there has been recent development in designs that employ techniques other than the traditional drive-wheel system for mobility.

The Walker

Perhaps the best method of providing mobility can be achieved by mimicking the solution nature has provided. While many forms of a "walking" robot exist, most apply the same concept of using articulated limbs that possess the ability for some degree of vertical and horizontal motion. The articulated walker is effective when properly functioning. However, the necessity for a sophisticated processor as well as numerous actuators makes these walkers relatively complex (Gates, 2004).

Methods for obtaining more simplistic walkers have been achieved using inexpensive electronic components (Hrynkiw and Tilden, 2002). The BEAM (Biology Electronics Aesthetics Mechanics) walking robot, as described by Hrynkiw and Tilden, achieves mobility by using two pairs of rigid legs shaped from copper wire. By eliminating articulated limbs from the design, the walker can function with only two servo motors to supply lift and thrust. Each pair of legs is fastened to a modified hobby servo motor. The servo motors can be arranged at varying angles with respect to each other to provide varying degrees of lift and thrust. Motor control is provided by a series of integrated circuits connected to a 6 V battery pack. A protruding wire "antenna" acts as a touch sensor. When triggered, the sensor will reverse the movement of the robot.

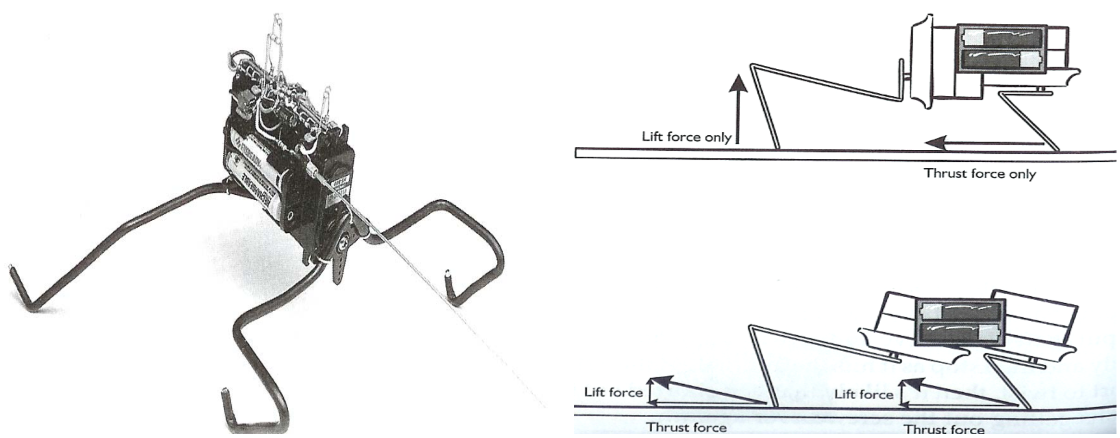

(a) (b)

Figure 5-9. (a) BEAM walker. (b) Diagram of various servo arrangements for varying lift and thrust (Hrynkiw and Tilden, 2002).

While the BEAM walker may not have the ability to be programmed to follow a predetermined path, it is capable of a primitive form of navigation. Much as the nervous system of an insect enables it to move throughout its environment, the basic sensor network of the walker will enable it to eventually find a suitable path through a field of obstacles. Additionally, small modifications can be made to the electronics and sensors to allow the walker to respond to other environmental stimuli, such as light.

An Array of Robots

One of the benefits provided by small robots, such as Hrynkiw and Tilden's BEAM walker, is the potential for creating robotic arrays. Small, simple robots are inexpensive, thus making them ideal for production in large quantities. While the random movements of an individual simple robot make it inefficient for use in surveillance or exploration, a large number of these robots could be used as a deployable sensor array. The individual random movements of a large number of robots could provide significant coverage of a location or structure.

One of the most fundamental limitations of small robots is the susceptibility to encountering impassable obstacles. Small objects, such as rocks and dirt, may not present a problem to large robots. However, these seemingly insignificant objects can pose great navigational challenges to small robots (Grabowski et al., 2003). One method for overcoming these obstacles is to create an array of robots that can collaborate to form a single unit when necessary.

Researchers are developing millibots (small robots) that can link together to form a chain in order to overcome large obstacles (Grabowski et al., 2003). Normally, each millibot functions as a small tracked vehicle and can usually climb over small objects.

However, if the group needs to maneuver around a large object, such as a flight of stairs, the millibots will join together to form a larger articulated unit. Unlike most conventional hitches, the millibot coupling joint contains a motor that can provide enough torque to lift several millibots. Thus, obstacles far greater in size than the individual millibot can be overcome by the group through collaboration as an articulated unit.

5.5 Conclusion

Mobile robotic systems have great potential for providing assistance in general surveillance tasks. From visual surveillance and long-term deployment in security operations, to victim identification and threat assessment at search and rescue sites, robotic systems may prove to be invaluable assets.

Structural health monitoring has already seen practical implementation of robotic systems. While many robotic technologies are still in development, the commercial production of various remote-control inspection units for structural health monitoring is evidence of the effectiveness of these systems. Robotics use may not be widespread, yet the commercialization of various pipe-crawlers, tank-inspectors, etc. suggests that widespread practical implementation of robotic systems may occur in the near future. While many of the current technologies employed may have limitations (e.g., remote-control, tethered systems), there is the potential for deployment of practical autonomous systems as well.

The development of the beam-crawler, as discussed in this paper, is an example of the potential application of autonomous robotic systems in structural health monitoring. The long-term deployment and continual surveillance of a structure provided by an autonomous inspection system could be far more cost-effective than employing human resources. The various inspection capabilities (visual, ultrasonic, etc.) and the enhanced accessibility provided by mobile robotic platforms might also improve the accuracy of structural integrity assessments.

There is no doubt that much progress is yet to be made in the development of complex autonomous systems before they can be widely implemented for a variety of tasks. Improvements in mobility as well as processing capabilities (e.g., image or object recognition) are necessary before robotic systems can be deployed without human guidance. However, based on the continuing advances in robotic technology and the evidence of potential benefits provided by robots, implementation of fully autonomous systems may soon be realized.

Works Cited

Arms, Steven. "Robotic Systems for Network Interrogation of Smart Civil Structures". NSF Small Business Innovation Research Program Proposal. Burlington, VT: Microstrain, Inc. 1999.

Becker, Jens, Laurence J. Jacobs, and Jianmin Qu. "Characterization of Cement-Based Materials Using Diffuse Ultrasound". Journal of Engineering Mechanics December 2003: 1478-1484.

Dolan, John, et al. Distributed Tactical Surveillance with ATVs. Proc. *SPIE* Conference on Unmanned Ground Vehicle Technology (Aerosense 1999). Vol. 3693. Bellingham, WA: *SPIE* 1999.

Envirosight, Inc. 111 Canfield Ave., Randolph, NJ 07869.

Esser, Brian, et al. Wireless Inductive Robotic Inspection of Structures. Proc. *IASTED* 2000 International Conference. 14-16 August 2000. Honolulu: 2000.

Federal Energy Regulatory Commission. Division of Dam Safety and Inspections Operating Manual. Washington D.C.: Federal Energy Regulatory Commission Division of Dam Safety, 2003.

Federal Highway Administration. Reliability of Visual Inspection for Highway Bridges, Vol. I (FHWA-RD-01-020). McLean, VA: Federal Highway Administration Research Center, 2001.

Federal Highway Administration (2002a). Status of the Nation's Highways, Bridges, and Transit: Conditions and Performance Report to Congress. McLean, VA: Federal Highway Administration Research Center, 2002.

Federal Highway Administration (2002b). Bridge Inspector's Reference Manual, Vol. I&II (FHWA NHI 03-001). McLean, VA: 2002.

Fortner, Brian. "Embedded Miniature Sensors Detect Chloride in Bridge Decks". Civil Engineering Vol. 73. No. 6. June 2003: 42-43.

Fowler, et al. Theory and Application of Precision Ultrasonic Thickness Gauging. USA: General Electric Company, 2003.

GE Panametrics. Ultrasonic Transducer Technical Notes. USA: General Electric Company, 2003.

Gates, Dan. "Personal Robotics: Instant Walker". Nuts and Volts. Jan. 2004: 21-24.

Grabowski, Robert, Luis E. Navarro-Serment, and Pradeep K. Khosla. "An Army of Small Robots". Scientific American Nov. 2003: 63-67.

Hrynkiw, Dave, and Mark W. Tilden. Junkbots, Bugbots, & Bots on Wheels: Building Simple Robots with BEAM Technology. Berkeley, CA: McGraw-Hill/Osborne, 2002.

Hudson, Kurt. LabVIEW-controlled Robot Climbs and Inspects Highway Lighting Towers. National Instruments Corporation, 2002.

Huston, Dryver, et al. Robotic and Mobile Sensor Systems for Structural Health Monitoring. Paper presented at the *ISHWM* 2003 Conference. 2003.

Kantor, G.A., et al. Collection of Environmental Data From an Airship Platform. Proc. *SPIE* Conference on Sensor Fusion and Decentralized Control in Robotic Systems IV. Vol. 4571. Bellingham, WA: *SPIE*, 2001.

Microstrain, Inc. 310 Hurricane Lane, Suite 4. Williston, VT 05495.

Murphy, Robin, et al. Mobility and Sensing Demands in USAR. Proc. IEEE International Conference on Industrial Electronics, Control, and Instrumentation (SS5-RE-4). Oct. 2000.

Taha, Mahmoud Reda, Husam Kinawi, and Naser El-Sheimy. The Realization of Commercial Structural Health Monitoring Using Information Technology Based Techniques. Proc. *SHM ISIS* 2002 Workshop. 2002.

Trebi-Ollennu, Ashitey, and Brett Kennedy. "Minirovers as Test Beds for Robotic Sensor-Web Concepts Fido Rover". *NASA* Tech Brief. Vol. 26. No. 11. Pasadena, CA: *NASA* Jet Propulsion Laboratory, 2002.

Turner, A. "Development of a Semi-Autonomous Control System for the *UVA* Solar Airship". Progress Report from *UVA* Solar Airship Program. Charlottesville, VA: University of Virginia.

United States Army Corps of Engineers. Fury – An Underground Tank Inspection System (Fact Sheet). Champaign, IL: U.S. Army Corps of Engineers Construction and Engineering Research Laboratory, 1999.

United States Army Corps of Engineers. Robotic Inspection System of Buried and Submerged Structures. Champaign, IL: U.S. Army Corps of Engineers Construction Engineering Research Laboratory, 2001.

United States Government. Pipeline Safety: Pipeline Integrity Management in High Consequence Areas (Gas Transmission Pipelines); Proposed Rule. (49 CFR Part 192). Federal Register. Vol. 68. No. 18. U.S. National Archives and Records Administration: January 28, 2003.

United States Government. National Bridge Inspection Standards. Code of Federal Regulations (Title 23, Chapter I 650.301-650.311). U.S. National Archives and Records Administration: Revised April 1, 2002.

Woo, Dah-Cheng. "Robotics in Highway Construction and Maintenance". Public Roads Vol. 58. No. 3. Online. Internet. Winter 1995.

Virginia Technologies, Inc. 2015 Ivy Road, Suite 423, Charlottesville, VA 22903.